

1 **A global hotspot for dissolved organic carbon in hypermaritime watersheds of coastal**  
2 **British Columbia.**

3  
4 Allison A. Oliver<sup>1,2</sup>, Suzanne E. Tank<sup>1,2</sup>, Ian Giesbrecht<sup>2,7</sup>, Maartje C. Korver<sup>2</sup>, William C.  
5 Floyd<sup>3,4,2</sup>, Paul Sanborn<sup>5,2</sup>, Chuck Bulmer<sup>6</sup>, Ken P. Lertzman<sup>7,2</sup>

6  
7 <sup>1</sup>University of Alberta, Department of Biological Sciences, CW 405, Biological Sciences Bldg.,  
8 University of Alberta, Edmonton, Alberta, T6G 2E9, Canada

9 <sup>2</sup>Hakai Institute, Tula Foundation, Box 309, Heriot Bay, British Columbia, V0P 1H0, Canada

10 <sup>3</sup>Ministry of Forests, Lands and Natural Resource Operations, 2100 Labieux Rd, Nanaimo, BC,  
11 V9T 6E9, Canada

12 <sup>4</sup>Vancouver Island University, 900 Fifth Street, Nanaimo, BC, V9R 5S5, Canada

13 <sup>5</sup>Ecosystem Science and Management Program, University of Northern British Columbia, 3333  
14 University Way, Prince George, BC, V2N 4Z9, Canada

15 <sup>6</sup>BC Ministry of Forests Lands and Natural Resource Operations, 3401 Reservoir Rd, Vernon,  
16 BC, V1B 2C7, Canada

17 <sup>7</sup>School of Resource and Environmental Management, Simon Fraser University, TASC 1- Room  
18 8405, 8888 University Drive, Burnaby, BC, V5A 1S6, Canada

19  
20  
21 Corresponding author: [aaoliver@ualberta.ca](mailto:aaoliver@ualberta.ca)

34 **Abstract**

35           The perhumid region of the coastal temperate rainforest (CTR) of Pacific North America  
36 is one of the wettest places on Earth and contains numerous small catchments that discharge  
37 freshwater and high concentrations of dissolved organic carbon (DOC) directly to the coastal  
38 ocean. However, empirical data on the flux and composition of DOC exported from these  
39 watersheds is scarce. We established monitoring stations at the outlets of seven catchments on  
40 Calvert and Hecate Islands, British Columbia, which represent the rain dominated hypermaritime  
41 region of the perhumid CTR. Over several years, we measured stream discharge, stream water  
42 DOC concentration, and stream water dissolved organic matter (DOM) composition. Discharge  
43 and DOC concentrations were used to calculate DOC fluxes and yields, and DOM composition  
44 was characterized using absorbance and fluorescence spectroscopy with parallel factor analysis  
45 (PARAFAC). The areal estimate of annual DOC yield in water year 2015 was 33.3 Mg C km<sup>-2</sup>  
46 yr<sup>-1</sup>, with individual watersheds ranging from an average of 24.1-37.7 Mg C km<sup>-2</sup> yr<sup>-1</sup>. This  
47 represents some of the highest DOC yields to be measured at the coastal margin. We observed  
48 seasonality in the quantity and composition of exports, with the majority of DOC export  
49 occurring during the extended wet period (September-April). Stream flow from catchments  
50 reacted quickly to rain inputs, resulting in rapid export of relatively fresh, highly terrestrial-like  
51 DOM. DOC concentration and measures of DOM composition were related to stream discharge  
52 and stream temperature, and correlated with watershed attributes, including the extent of lakes  
53 and wetlands, and thickness of organic and mineral soil horizons. Our discovery of high DOC  
54 yields from these small catchments in the CTR is especially compelling as they deliver relatively  
55 fresh, highly terrestrial organic matter directly to the coastal ocean. Hypermaritime landscapes  
56 are common on the British Columbia coast, suggesting that this coastal margin may play an

57 important role in the regional processing of carbon and in linking terrestrial carbon to marine  
58 ecosystems.

## 59 **1. Introduction**

60 Freshwater aquatic ecosystems process and transport a significant amount of carbon  
61 (Cole et al., 2007; Aufdenkampe et al., 2011; Dai et al., 2012). Globally, riverine export is  
62 estimated to deliver around 0.9 Pg C yr<sup>-1</sup> from land to the coastal ocean (Cole et al., 2007), with  
63 typically >50% quantified as dissolved organic carbon (DOC)(Meybeck, 1982; Ludwig et al.,  
64 1996; Alvarez-Cobelas et al., 2012; Mayorga et al., 2010). Rivers draining coastal watersheds  
65 serve as conduits of DOC from terrestrial and freshwater sources to marine environments  
66 (Mulholland and Watts, 1982; Bauer et al., 2013; McClelland et al., 2014) and can have  
67 important implications for coastal carbon cycling, biogeochemical interactions, ecosystem  
68 productivity, and food webs (Hopkinson et al., 1998; Tallis, 2009; Tank et al., 2012; Regnier et  
69 al., 2013). In addition, because the transfer of water and organic matter from watersheds to the  
70 coastal ocean represents an important pathway for carbon cycling and ecological subsidies  
71 between ecosystems, better understanding of these linkages is needed for constraining  
72 predictions of ecosystem productivity in response to perturbations such as climate change. In  
73 regions where empirical data are currently scarce, quantifying land-to-ocean DOC export is  
74 therefore a priority for improving the accuracy of watershed and coastal carbon models (Bauer et  
75 al., 2013).

76 While quantifying DOC flux within and across systems is required for understanding the  
77 magnitude of carbon exchange, the composition of DOC (as dissolved organic matter, or DOM)  
78 is also important for determining the ecological significance of carbon exported from coastal  
79 watersheds. The aquatic DOM pool is a complex mixture that reflects both source material and

80 processing along the watershed terrestrial-aquatic continuum, and as a result can show  
81 significant spatial and temporal variation (Hudson et al., 2007; Graeber et al., 2012; Wallin et al.,  
82 2015). Both DOC concentration and DOM composition can serve as indicators of watershed  
83 characteristics (Koehler et al., 2009), hydrologic flow paths (Johnson et al., 2011; Helton et al.,  
84 2015), and watershed biogeochemical processes (Emili and Price, 2013). DOM composition can  
85 also influence its role in downstream processing and ecological function, such as susceptibility to  
86 biological (Judd et al., 2006) and physiochemical interactions (Yamashita and Jaffé, 2008).

87         The coastal temperate rainforests (CTR) of Pacific North America extend from the Gulf  
88 of Alaska, through British Columbia, to Northern California and span a wide range of  
89 precipitation and climate regimes. Within this rainforest region, the “perhumid” zone has cool  
90 summers and summer precipitation is common (>10% of annual precipitation) (Alaback,  
91 1996)(Fig. 1). The perhumid CTR extends from southeast Alaska through the outer coast of  
92 central British Columbia and contains forests and soils that have accumulated large amounts of  
93 organic carbon above and below ground (Leighty et al., 2006; Gorham et al., 2012). Due to high  
94 amounts of precipitation and close proximity to the coast, this area represents a potential hotspot  
95 for the transport and metabolism of carbon across the land-to-ocean continuum, and quantifying  
96 these fluxes is pertinent for understanding global carbon cycling.

97         Within the large perhumid CTR, there is substantial spatial variation in climate and  
98 landscape characteristics that create uncertainty about carbon cycling and pattern. In Alaska, for  
99 example, riverine DOC concentrations vary with wetland cover (D’Amore et al. 2015a) and  
100 glacial cover (Fellman et al. 2014). Previous studies have shown that streams in southeast Alaska  
101 can contain high DOC concentrations (Fellman et al., 2009a; D’Amore et al., 2015a) and  
102 produce high DOC yields (D’Amore et al., 2015b; D’Amore et al., 2016, Stackpoole et al.,

103 2016), but no known field estimates have been generated for the perhumid CTR of British  
104 Columbia, an area of approximately 97,824 km<sup>2</sup> (adapted from Wolf et al., 1995). Within the  
105 perhumid CTR of British Columbia, terrestrial ecologists have defined a large (29,935 km<sup>2</sup>)  
106 *hypermaritime* sub-region where rainfall dominates over snow, seasonality is moderated by the  
107 ocean, and wetlands are extensive (Pojar et al., 1991; area estimated using British Columbia  
108 Biogeoclimatic Ecosystem Classification Subzone/Variant mapping Version 10, August 31,  
109 2016, available at: [https://catalogue.data.gov.bc.ca/dataset/f358a53b-ffde-4830-a325-](https://catalogue.data.gov.bc.ca/dataset/f358a53b-ffde-4830-a325-a5a03ff672c3)  
110 [a5a03ff672c3](https://catalogue.data.gov.bc.ca/dataset/f358a53b-ffde-4830-a325-a5a03ff672c3)). Previous work in the hypermaritime CTR showed that DOC concentrations are  
111 high in small streams and tend to increase during rain events (Gibson et al., 2000; Fitzgerald et  
112 al., 2003; Emili and Price, 2013). Taken together, these conditions should be expected to  
113 generate high yields and fluxes of DOC from hypermaritime watersheds to the coastal ocean.

114 The objectives of this study were to provide the first field-based estimates of DOC  
115 exports from watersheds in the extensive hypermaritime region of British Columbia's perhumid  
116 CTR, to describe the temporal and spatial dynamics of exported DOC concentration and DOM  
117 composition, and to identify relationships between DOC concentration, DOM composition, and  
118 watershed characteristics.

## 119 **2. Methods**

### 120 **2.1 Study Sites**

121 Study sites are located on northern Calvert Island and adjacent Hecate Island on the  
122 central coast of British Columbia, Canada (Lat 51.650, Long -128.035; Fig. 1). Average annual  
123 precipitation and air temperature at sea level from 1981-2010 was 3356 mm yr<sup>-1</sup> and 8.4 °C  
124 (average annual min= 0.9°C, average annual max= 17.9°C) (available online at  
125 <http://www.climatewna.com/>; Wang et al., 2012), with precipitation dominated by rain, and

126 winter snowpack persisting only at higher elevations. Sites are located within the hypermaritime  
127 region of the CTR on the outer coast of British Columbia. Soils overlying the granodiorite  
128 bedrock (Roddick, 1996) are usually < 1 m thick, and have formed in sandy colluvium and  
129 patchy morainal deposits, with limited areas of coarse glacial outwash. Chemical weathering and  
130 organic matter accumulation in the cool, moist climate have produced soils dominated by  
131 Podzols and Follic Histosols, with Hemists up to 2 m thick in depressional sites (IUSS Working  
132 Group WRB, 2015). The landscape is comprised of a mosaic of ecosystem types, including  
133 exposed bedrock, extensive wetlands, bog forests and woodlands, with organic rich soils (Green,  
134 2014; Thompson et al., 2016). Forest stands are generally short with open canopies reflecting the  
135 lower productivity of the hypermaritime forests compared to the rest of the perhumid CTR  
136 (Banner et al., 2005). Dominant trees are western redcedar, yellow-cedar, shore pine and western  
137 hemlock with composition varying across topographic and edaphic gradients. Widespread  
138 understory plants include bryophytes, salal, deer fern, and tufted clubmoss. Wetland plants are  
139 locally abundant including diverse *Sphagnum* mosses and sedges. Although the watersheds have  
140 no history of mining or industrial logging, archaeological evidence suggests that humans have  
141 occupied this landscape for at least 13,000 years (McLaren et al., 2014). This occupation has had  
142 a local effect on forest productivity near habitation sites (Trant et al., 2016) and on fire regimes  
143 (Hoffman et al., 2016). We selected seven watersheds with streams draining directly into the  
144 ocean (Fig. 1). These numbered watersheds (626, 693, 703, 708, 819, 844, and 1015) range in  
145 size (3.2 to 12.8 km<sup>2</sup>) and topography (maximum elevation 160 m to 1012 m), are variably  
146 affected by lakes (0.3 – 9.1% lake coverage), and – as is characteristic of the perhumid CTR –  
147 have a high degree of wetland coverage (24– 50%) (Table 1).

## 148 **2.2 Soils and watershed characteristics**

149 Watersheds and streams were delineated using a 3 m resolution digital elevation model  
150 (DEM) derived from airborne laser scanning (LiDAR) and flow accumulation analysis using  
151 geographic information systems (GIS) to summarize watershed characteristics for each  
152 watershed polygon and for all watersheds combined (Gonzalez Arriola et al., 2015; Table 1).  
153 Topographic measures were estimated from the DEM, and lake and wetland cover estimated  
154 from Province of British Columbia Terrestrial Ecosystem Mapping (TEM) (Green, 2014), and  
155 soil material thickness estimated from unpublished digital soil maps (Supplemental S1). We  
156 recorded thickness of organic soil material, thickness of mineral soil material, and total soil depth  
157 to bedrock at a total of 353 field sites. Mineral soil horizons have  $\leq 17\%$  organic C, while  
158 organic soil horizons have  $> 17\%$  organic C, per the Canadian System of Soil Classification (Soil  
159 Classification Working Group, 1998). In addition to field-sampled sites, 40 sites with exposed  
160 bedrock (0 cm soil depth) were located using aerial photography. Soil thicknesses were  
161 combined with a suite of topographic, vegetation, and remote sensing (LiDAR and RapidEye  
162 satellite imagery) data for each sampling point and used to train a random forest model  
163 (randomForest package in R; Liaw and Wiener, 2002) that was used to predict soil depth values.  
164 Soil material thicknesses were then averaged for each watershed (Table 1). For additional details  
165 on field site selection and methods used for predictions of soil thickness, see Supplemental S1.1.

### 166 **2.3 Sample Collection and Analysis**

167 From May 2013 to July 2016, we collected stream water grab samples from each  
168 watershed stream outlet every 2-3 weeks ( $n_{\text{total}} = 402$ ), with less frequent sampling ( $\sim$  monthly)  
169 during winter (Fig. 1). All samples were filtered in the field (Millipore Millex-HP Hydrophilic  
170 PES 0.45 $\mu\text{m}$ ) and kept in the dark, on ice until analysis. DOC samples were filtered into 60 mL  
171 amber glass bottles and preserved with 7.5M  $\text{H}_3\text{PO}_4$ . Fe samples were filtered into 125 mL

172 HDPE bottles and preserved with 8M HNO<sub>3</sub>. DOC and Fe samples were analyzed at the BC  
173 Ministry of the Environment Technical Services Laboratory (Victoria, BC, Canada). DOC  
174 concentrations were determined on a TOC analyzer (Aurora 1030; OI-Analytical) using wet  
175 chemical oxidation with persulfate followed by infrared detection of CO<sub>2</sub>. Fe concentrations  
176 were determined on a dual-view ICP-OES spectrophotometer (Prodigy; Teledyne Leeman Labs)  
177 using a Seaspray pneumatic nebulizer.

178 In May 2014, we began collecting stream samples for stable isotopic composition of  $\delta^{13}\text{C}$   
179 in DOC ( $\delta^{13}\text{C}$ -DOC; n= 173) and optical characterization of DOM using absorbance  
180 spectroscopy (n= 259). Beginning in January 2016, we also analyzed samples using fluorescence  
181 spectroscopy (see section 2.6). Samples collected for  $\delta^{13}\text{C}$ -DOC were filtered into 40 mL EPA  
182 glass vials and preserved with H<sub>3</sub>PO<sub>4</sub>.  $\delta^{13}\text{C}$ -DOC samples were analyzed at GG Hatch Stable  
183 Isotope Laboratory (Ottawa, ON, Canada) using high temperature combustion (TIC-TOC  
184 Combustion Analyser Model 1030; OI Analytical) coupled to a continuous flow isotope ratio  
185 mass spectrometry (Finnigan Mat DeltaPlusXP; Thermo Fischer Scientific)(Lalonde et al. 2014).  
186 Samples analyzed for optical characterization using absorbance and fluorescence were filtered  
187 into 125 mL amber HDPE bottles and analyzed at the Hakai Institute (Calvert Island, BC,  
188 Canada) within 24 hours of collection.

#### 189 **2.4 Hydrology: Precipitation and Stream Discharge**

190 We measured precipitation using a TB4-L tipping bucket rain gauge with a 0.2 mm  
191 resolution (Campbell Scientific Ltd.) located in watershed 708 (elevation= 16 m a.s.l). The rain  
192 gauge was calibrated twice per year using a Field Calibration Device, model 653 (HYQUEST  
193 Solutions Ltd).



194 We determined continuous stream discharge for each watershed by developing stage  
195 discharge rating curves at fixed hydrometric stations situated in close proximity to each stream  
196 outlet. Sites were located above tidewater influence and were selected based on favourable  
197 conditions (i.e., channel stability and stable hydraulic conditions) for the installation and  
198 operation of pressure transducers to measure stream stage. From August 2014 to May 2016 (21  
199 months), we measured stage every 5 minutes using an OTT PLS –L (OTT Hydromet, Colorado,  
200 USA) pressure transducer (0-4 m range SDI-12) connected to a CR1000 (Campbell Scientific,  
201 Edmonton, Canada) data logger. Stream discharge was measured over various intervals using  
202 either the velocity area method (for flows  $< 0.5 \text{ m}^3\text{s}^{-1}$ ; ISO Standard 9196:1992, ISO Standard  
203 748:2007) or salt dilution (for flows  $> 0.5 \text{ m}^3\text{s}^{-1}$ ; Moore, 2005). Rating curves were developed  
204 using the relationship between stream stage height and stream discharge (Supplemental S2).

## 205 **2.5 DOC flux**

206 From October 1, 2014 to April 30, 2016, we estimated DOC flux for each watershed  
207 using measured DOC concentrations (n= 224) and continuous discharge recorded at 15-minute  
208 intervals. The watersheds in this region respond rapidly to rain inputs and as a result DOC  
209 concentrations are highly variable. To address this variability, routine DOC concentration data  
210 (as described in section 2.2) were supplemented with additional grab samples (n= 21) collected  
211 around the peak of the hydrograph during several high flow events throughout the year. We  
212 performed watershed-specific estimates of DOC flux using the “rloadest” package (Lorenz et al.,  
213 2015) in R (version 3.2.5, R Core Team, 2016), which replicates functions developed in the U.S.  
214 Geological Survey load-estimator program, LOADEST (Runkel et al., 2004). LOADEST is a  
215 multiple-regression adjusted maximum likelihood estimation model that calibrates a regression  
216 between measured constituent values and stream flow across seasons and time and then fits it to

217 combinations of coefficients representing nine predetermined models of constituent flux. To  
218 account for potentially small sample size, the best model was selected using the second order  
219 Akaike Information Criterion (AICc) (Akaike, 1981; Hurvich and Tsai, 1989). Input data were  
220 log-transformed to avoid bias and centered to reduce multicollinearity. For additional details on  
221 model selection, see Supplemental Table S3.1.

## 222 **2.6 Optical characterization of DOM**

223 Prior to May 2014, absorbance measures of water samples (n= 99) were conducted on a  
224 Varian Cary-50 (Varian, Inc.) spectrophotometer at the BC Ministry of the Environment  
225 Technical Services Laboratory (Victoria, BC, Canada) to determine specific UV absorption at  
226 254 nm (SUVA<sub>254</sub>). After May 2014, we conducted optical characterization of DOM by  
227 absorbance and fluorescence spectroscopy at the Hakai Institute field station (Calvert Island, BC,  
228 Canada) using an Aqualog fluorometer (Horiba Scientific, Edison, New Jersey, USA). Strongly  
229 absorbing samples (absorbance units > 0.2 at 250 nm) were diluted prior to analysis to avoid  
230 excessive inner filter effects (Lakowicz, 1999). Samples were run in 1 cm quartz cells and  
231 scanned from 220-800 nm at 2 nm intervals to determine SUVA<sub>254</sub> as well as the spectral slope  
232 ratio ( $S_R$ ). SUVA<sub>254</sub> has been shown to positively correlate with increasing molecular aromaticity  
233 associated with the fulvic acid fraction of DOM (Weishaar et al., 2003), and is calculated by  
234 dividing the Decadic absorption coefficient at 254 nm by DOC concentration (mg C L<sup>-1</sup>). To  
235 account for potential Fe interference with absorbance values, we corrected SUVA<sub>254</sub> values by Fe  
236 concentration according the method described in Poulin et al., (2014).  $S_R$  has been shown to  
237 negatively correlate with molecular weight (Helms et al., 2008), and is calculated as the ratio of  
238 the spectral slope from 275 nm to 295 nm ( $S_{275-295}$ ) to the spectral slope from 350 nm to 400 nm  
239 ( $S_{350-400}$ ).

240 We measured excitation and emission spectra (as excitation emission matrices, EEMs) on  
241 samples every three weeks from January to July 2016 (n= 63). Samples were run in 1 cm quartz  
242 cells and scanned from excitation wavelengths of 230-550 nm at 5nm increments, and emission  
243 wavelengths of 210-620 nm at 2 nm increments. The Horiba Aqualog applied the appropriate  
244 instrument corrections for excitation and emission, inner filter effects, and Raman signal  
245 calibration. We calculated the Fluorescence Index and Freshness Index for each EEM. The  
246 Fluorescence Index is often used to indicate DOM source, where higher values are more  
247 indicative of microbial-derived sources of DOM and lower values indicate more terrestrial-  
248 derived sources (McKnight et al., 2001), and is calculated as the ratio of emission intensity at  
249 450 nm to 500 nm, at an excitation of 370 nm. The Freshness Index is used to indicate the  
250 contribution of autochthonous or recently microbial-produced DOM, with higher values  
251 suggesting greater autochthony (i.e., microbial inputs), and is calculated as the ratio of emission  
252 intensity at 380 nm to the maximum emission intensity between 420 nm and 435 nm, at  
253 excitation 310 nm (Wilson and Xenopoulos, 2009).

254 To further characterize features of DOM composition, we performed parallel factor  
255 analysis (PARAFAC) using EEM data within the drEEM toolbox for Matlab (Mathworks, MA,  
256 USA) (Murphy et al., 2013). PARAFAC is a statistical technique used to decompose the  
257 complex mixture of the fluorescing DOM pool into quantifiable, individual components  
258 (Stedmon et al., 2003). We detected a total of six unique components, and validated the model  
259 using core consistency and split-half analysis (Murphy et al., 2013; Stedmon and Bro, 2008).  
260 Components with similar spectra from previous studies were identified using the online  
261 fluorescence repository, OpenFluor (Murphy et al., 2014), and additional components with  
262 similar peaks were identified through literature review. Since the actual chemical structure of

263 fluorophores is unknown, we used the concentration of each fluorophore as maximum  
264 fluorescence of excitation and emission in Raman Units ( $F_{\max}$ ) to derive the percent contribution  
265 of each fluorophore component to total fluorescence. Relationships between PARAFAC  
266 components were also evaluated using Pearson correlation coefficients in the R package “Hmisc”  
267 (Harrell et al., 2016).

## 268 **2.7 Evaluating relationships in DOC concentration and DOM composition with stream** 269 **discharge and temperature**

270 We used linear mixed effects models to assess the relationship between DOC  
271 concentration or DOM composition ( $\delta^{13}\text{C}$ -DOC,  $S_R$ , SUVA<sub>254</sub>, Fluorescence Index, Freshness  
272 Index, PARAFAC components), stream discharge, and stream temperature. Analysis was  
273 performed in R using the nlme package (Pinheiro et al., 2016). Watershed was included as a  
274 random intercept to account for repeat measures on each watershed. For some parameters, a  
275 random slope of either discharge or temperature was also included based on data assessment and  
276 model selection. Model selection was performed using AIC to compare models fit using  
277 Maximum Likelihood (ML) (Burnham and Anderson, 2002; Symonds and Moussalli, 2010). The  
278 final model was fit using Restricted Maximum Likelihood (REML). Marginal  $R^2$ , which  
279 represents an approximation of the proportion of the variance explained by the fixed factors  
280 alone, and conditional  $R^2$ , which represents an approximation of the proportion of the variance  
281 explained by both the fixed and random factors, were calculated based on the methods described  
282 in Nakagawa and Schielzeth (2013) and Johnson (2014).

## 283 **2.8 Redundancy analysis: Relationships between DOC concentration, DOM composition,** 284 **and watershed characteristics**

285 We evaluated relationships between stream water DOC and watershed characteristics by  
286 relating DOC concentration and measures of DOM composition to catchment attributes using  
287 redundancy analysis (RDA; type 2 scaling) in the package `rdaTest` (Legendre and Durand, 2014)  
288 in R (version 3.2.2, R Core Team, 2015). To maximize the amount of information available, we  
289 performed RDA analysis on samples collected from January to July 2016, and therefore included  
290 all parameters of optical characterization (i.e., all PARAFAC components and spectral indices).  
291 We assessed the collinearity of DOM compositional variables using a variance inflation factor  
292 (VIF) criteria of  $> 10$ , which resulted in the removal of PARAFAC components C2, C3, and C5  
293 prior to RDA analysis. Catchment attributes for each watershed included average slope, percent  
294 area of lakes, percent area of wetlands, average depth of mineral soil, and average depth of  
295 organic soil. Relationships between variables were linear, so no transformations were necessary  
296 and variables were standardized prior to analysis. To account for repeat monthly measures per  
297 watershed and potential temporal correlation associated with monthly sampling, we included  
298 sample month as a covariable (“partial-RDA”). To test whether the RDA axes significantly  
299 explained variation in the dataset, we compared permutations of residuals using ANOVA (9,999  
300 iterations; `test.axes` function of `rdaTest`).

### 301 **3. Results**

#### 302 **3.1 Hydrology**

303 We present work for water year 2015 (WY2015; October 1, 2014 – September 30, 2015)  
304 and water year 2016 (WY2016; October 1, 2015 – September, 30, 2016). Annual precipitation  
305 for both water years was lower than historical mean annual precipitation (WY2015= 2661 mm;  
306 WY2016= 2587 mm). It is worth noting that mean annual precipitation at our rain gauge location  
307 (2890 mm yr<sup>-1</sup>, elevation = 16 m) is substantially lower than the average amount received at

308 higher elevations, which from 1981-2010 was approximately  $5027 \text{ mm yr}^{-1}$  at an elevation of  
309 1000m within our study area. This area receives a very high amount of annual rainfall but also  
310 experiences seasonal variation, with an extended wet period from fall through spring, and a much  
311 shorter, typically drier period during summer. In WY2015 and WY2016, 86-88% of the annual  
312 precipitation on Calvert Island occurred during the 8-months of wetter and cooler weather  
313 between September and April (~ 75% of the year), designated the “wet period” (WY2015 wet=  
314 2388 mm, average air temp=  $7.97^{\circ}\text{C}$ ; WY2016 wet= 2235 mm; average air temp=  $7.38^{\circ}\text{C}$ ). The  
315 remaining annual precipitation occurred during the drier and warmer summer months of May –  
316 August, designated the “dry period” (WY2015 dry= 314 mm, average air temp=  $13.4^{\circ}\text{C}$ ;  
317 WY2016 dry= 352 mm, average air temp=  $13.1^{\circ}\text{C}$ ). Overall, although WY2015 was slightly  
318 wetter than WY2016, the two years were comparable in relative precipitation during the wet  
319 versus dry periods.

320 Stream discharge (Q) responded rapidly to rain events and as a result, closely tracked  
321 patterns in total precipitation (Fig. 2). Total Q for all watersheds was on average 22% greater for  
322 the wet period of WY2015 (total Q=  $223.02 * 10^6$ ; range=  $5.13 * 10^6 - 111.51 * 10^6 \text{ m}^3$ )  
323 compared to the wet period of WY2016 (total Q=  $182.89 * 10^6$ ; range=  $4.17 * 10^6 - 91.45 * 10^6$   
324  $\text{m}^3$ ). Stream discharge and stream temperature were significantly different for wet versus dry  
325 periods (Mann-Whitney tests,  $p < 0.0001$ ).

### 326 **3.2 Temporal and spatial patterns in DOC concentration, yield and flux**

327 Stream waters were high in DOC concentration relative to the global average for  
328 freshwater discharged directly to the ocean (average DOC for Calvert and Hecate Islands =  $10.4$   
329  $\text{mg L}^{-1}$ , std= 3.8; average global DOC=  $\sim 6 \text{ mg L}^{-1}$ ) (Meybeck, 1982; Harrison et al., 2005)  
330 (Table 1; Fig. 3). Q-weighted average DOC concentrations were higher than average measured

331 DOC concentrations ( $11.1 \text{ mg L}^{-1}$ , Table 1), and also resulted in slightly different ranking of the  
332 watersheds for highest to lowest DOC concentration. Within watersheds, Q-weighted DOC  
333 concentrations ranged from a low of  $8.4 \text{ mg L}^{-1}$  (watershed 693) to a high of  $19.3 \text{ mg L}^{-1}$   
334 (watershed 819), and concentrations were significantly different between watersheds (Kruskal-  
335 Wallis test,  $p < 0.0001$ ). Seasonal variability tended to be higher in watersheds where DOC  
336 concentration was also high (watersheds 626, 819, and 844) and lower in watersheds with greater  
337 lake area (watersheds 1015 and 708) (Table 1; box plots, Figure 3). On an annual basis, DOC  
338 concentrations generally decreased through the wet period, and increased through the dry period,  
339 and concentrations were significantly lower during the wet period compared to the dry period  
340 (Mann-Whitney test,  $p = 0.0123$ ). Results of our linear mixed effects (LME) model  
341 (Supplemental Table S6.1) indicate that DOC concentration was positively related to both  
342 discharge ( $b = 0.613$ ,  $p < 0.001$ ) and temperature ( $b = 0.162$ ,  $p = 0.011$ ) (model conditional  $R^2 =$   
343  $0.57$ , marginal  $R^2 = 0.09$ ).

344 Annual and monthly DOC yields are presented in Table 1. For the total period of  
345 available Q (October 1, 2014 - April 30, 2016; 19 months), areal (all watersheds) DOC yield was  
346  $52.3 \text{ Mg C km}^{-2}$  (95% CI= 45.7 to  $68.2 \text{ Mg C km}^{-2}$ ) and individual watershed yields ranged from  
347 24.1 to  $43.6 \text{ Mg C km}^{-2}$ . For WY2015, areal annual DOC yield was  $33.3 \text{ Mg C km}^{-2} \text{ yr}^{-1}$  (95%  
348 CI= 28.9 to  $38.1 \text{ Mg C km}^{-2} \text{ yr}^{-1}$ ). Total monthly rainfall was strongly correlated with monthly  
349 DOC yield (Fig. 4), and average monthly yield for the wet period ( $3.35 \text{ Mg C km}^{-2} \text{ mo}^{-1}$ ; 95%  
350 CI= 2.94 to  $4.40 \text{ Mg C km}^{-2} \text{ mo}^{-1}$ ) was significantly greater than average monthly yield during  
351 the dry period ( $0.50 \text{ Mg C km}^{-2} \text{ mo}^{-1}$ ; 95% CI= 0.41 to  $0.62 \text{ Mg C km}^{-2} \text{ mo}^{-1}$ ) (Mann-Whitney  
352 test,  $p < 0.0001$ ).

353 Across our study watersheds, DOC flux generally increased with increasing watershed  
354 area (Fig. 5). In WY2015, total DOC flux for all watersheds included in our study was 1562 Mg  
355 C (95% CI= 1355 to 1787 Mg C), and individual watershed flux ranged from 82 to  
356 276 Mg C. DOC flux was significantly different in wet versus dry periods (Mann-Whitney test,  $p$   
357  $< 0.0001$ ). Overall, 94% of the export in WY2015 occurred during the wet period, and export for  
358 the wet period of WY2015 was lower than export for the wet period of WY2016 (Fig. 5).

### 359 **3.3 Temporal and spatial patterns in DOM composition**

360 The stable isotopic composition of dissolved organic carbon ( $\delta^{13}\text{C}$ -DOC) was relatively  
361 tightly constrained over space and time (average  $\delta^{13}\text{C}$ -DOC=  $-26.53\text{‰}$ , std= 0.36; range= -  
362  $27.67\text{‰}$  to  $-24.89\text{‰}$ ). Values of  $S_R$  were low compared to the range typically observed in surface  
363 waters (average  $S_R = 0.78$ , std= 0.04; range= 0.71 to 0.89) and Fe-corrected  $\text{SUVA}_{254}$  values  
364 were at the high end of the range compared to most surface waters (average  $\text{SUVA}_{254}$  for Calvert  
365 and Hecate Islands=  $4.42 \text{ L mg}^{-1} \text{ m}^{-1}$ , std= 0.46; range of  $\text{SUVA}_{254}$  in surface waters = 1.0 to 5.0  
366  $\text{L mg}^{-1} \text{ m}^{-1}$ ) (Spencer et al., 2012). Values for both Fluorescence Index (average Fluorescence  
367 Index= 1.36, std= 0.04; range= 1.30 to 1.44) and Freshness Index (average Freshness Index=  
368 0.46, std= 0.02; range= 0.41 to 0.49) were relatively low compared to the typical range found in  
369 surface waters (Fellman et al., 2010; Hansen et al., 2016). Differences between watersheds were  
370 observed for  $\delta^{13}\text{C}$ -DOC (Kruskal-Wallis test,  $p= 0.0043$ ),  $S_R$  (Kruskal-Wallis test,  $p= 0.0001$ ),  
371 Fluorescence Index (Kruskal-Wallis test,  $p= 0.0030$ ), and Freshness Index (Kruskal-Wallis test,  
372  $p= 0.0099$ ), but watersheds did not differ in  $\text{SUVA}_{254}$  (Kruskal-Wallis test,  $p= 0.4837$ ).

373 We observed seasonal variability in  $\delta^{13}\text{C}$ -DOC throughout the period of sample (Fig. 3  
374 and our LME model (Supplemental Table S6.1) indicate that  $\delta^{13}\text{C}$ -DOC declined with increasing  
375 discharge ( $b= -0.049$ ,  $p= 0.014$ ) and stream temperature ( $b= -0.024$ ,  $p< 0.001$ ) (model



376 conditional  $R^2= 0.35$ , marginal  $R^2= 0.10$ ). In contrast, although  $SUVA_{254}$  appeared to exhibit a  
377 general seasonal trend of values increasing over the wet period and decreasing over the dry  
378 period,  $SUVA_{254}$  was not significantly related to either discharge or stream temperature in the  
379 LME model results.  $S_R$  also appeared to fluctuate seasonally, with lower values during the wet  
380 season and higher values during the dry season.  $S_R$  was negatively related to discharge ( $b= -$   
381  $0.026$ ,  $p< 0.001$ ) and positively related to the interaction between discharge and stream  
382 temperature ( $b= 0.0015$ ,  $p< 0.001$ ) (model conditional  $R^2= 0.62$ , marginal  $R^2= 0.28$ ). Freshness  
383 Index was negatively related to stream temperature ( $b= -0.003$ ,  $p= 0.008$ ) (model conditional  $R^2=$   
384  $0.59$ , marginal  $R^2= 0.23$ ), while Fluorescence Index was not significantly related to either  
385 discharge or stream temperature.

### 386 **3.4 PARAFAC characterization of DOM**

387 Six fluorescence components were identified through PARAFAC (“C1” through “C6”)  
388 (Table 2). Additional details on PARAFAC model results are provided in Supplemental Table  
389 S4.1, Fig. S4.2, and Fig. S4.3. Of the six components, four were found to have close spectral  
390 matches in the OpenFluor database (C1, C3, C5, C6; minimum similarity score  $> 0.95$ ), while  
391 the remaining two (C2 and C4) were found to have similar peaks represented in the literature.  
392 The first four components (C1 through C4) are described as terrestrial-derived, whereas  
393 components C5 and C6 are described as autochthonous or microbially-derived (Table 2). In  
394 general, the rank order of each components’ percent contribution to total fluorescence was  
395 maintained over time, with C1 comprising the majority of total fluorescence across all  
396 watersheds (Fig. 6).

397 Across watersheds, components fluctuated synchronously over time and variation  
398 between watersheds was relatively low, although slightly more variation between watersheds

399 was observed during the beginning of the dry period relative to other times of the year (Fig 6).  
400 The percent contributions of components C1, C3, C5 and C6 to total fluorescence were not  
401 significantly different across watersheds (for all components Kruskal-Wallis test,  $p > 0.05$ ),  
402 however percent composition of both C2 and C4 were different (Kruskal-Wallis test,  $p = 0.0306$   
403 and  $p = 0.0307$ , respectively) and higher for watersheds 819 and 844 relative to the other  
404 watersheds (Supplemental Fig. S4.4).

405 PARAFAC components exhibited significant relationships with stream discharge and  
406 stream temperature, although predicted changes (beta, or  $b$ ) in fluorescence components with  
407 discharge and/or stream temperature were small (Supplemental Table S6.2). C3 increased with  
408 discharge ( $b = 0.006$ ,  $p = 0.003$ ), whereas C2, C4, and C5 decreased with discharge (C2:  $b = -$   
409  $0.005$ ,  $p = 0.022$ ; C4:  $b = -0.008$ ,  $p = 0.002$ ; C5:  $b = -0.008$ ,  $p = 0.002$ ). C1, C4, and C6 increased  
410 with temperature (C1:  $b = 0.001$ ,  $p = 0.050$ ; C4:  $b = 0.003$ ,  $p < 0.001$ ; C6:  $b = 0.005$ ,  $p = 0.005$ ),  
411 while both C3 and C5 decreased with temperature (C3:  $b = -0.003$ ,  $p = 0.003$ ; C5:  $b = -0.003$ ,  $p =$   
412  $0.027$ ). Conditional  $R^2$  values for the models ranged from 0.28 to 0.69, while marginal  $R^2$  ranged  
413 from 0.20 to 0.46. Overall, greater changes in component contribution to total fluorescence were  
414 observed with changes in discharge relative to changes in stream temperature.

### 415 **3.5 Relationships between watershed characteristics, DOC concentrations, and DOM** 416 **composition**

417 Results of the partial-RDA (type 2 scaling) were significant in explaining variability in  
418 DOM concentration and composition (semi-partial  $R^2 = 0.33$ ,  $F = 7.90$ ,  $p < 0.0001$ ) (Fig. 7). Axes  
419 1 through 3 were statistically significant at  $p < 0.001$ , and the relative contribution of each axis to  
420 the total explained variance was 47%, 30%, and 22%, respectively. Additional details on the  
421 RDA test are provided in Supplemental Figs. S5.1-S5.2 and Tables S5.3 – S5.5. Axis 1 described

422 a gradient of watershed coverage by water-inundated ecosystem types, ranging from more  
423 wetland coverage to more lake coverage. Total lake coverage (area) and mean mineral soil  
424 material thickness showed a strong positive contribution, and wetland coverage (area) showed a  
425 strong negative contribution to this axis. Freshness Index, Fluorescence Index,  $S_R$  and  
426 fluorescence component C6 were positively correlated with Axis 1, while component C4 showed  
427 a clear negative correlation. Axis 2 described a subtler gradient of soil material thickness ranging  
428 from greater mean organic soil material thickness to greater mean mineral soil material  
429 thickness. DOC concentration,  $\delta^{13}\text{C-DOC}$ ,  $\text{SUVA}_{254}$ , and fluorescence component C1 all showed  
430 a strong, positive correlation with Axis 2. Axis 3 described a gradient of watershed steepness,  
431 from lower gradient slopes with more wetland area and thicker organic soil material to steeper  
432 slopes with less developed organic horizons. Average slope contributed negatively to Axis 3 (see  
433 Supplemental Table S5.5), followed by positive contributions from both wetland area and  
434 thickness of organic soil material.  $\delta^{13}\text{C-DOC}$  showed the most positive correlation with Axis 3,  
435 whereas fluorescence components C1 and C4 showed the most negative.

#### 436 **4. Discussion**

##### 437 **4.1 DOC export from small catchments to the coastal ocean**

438 In comparison to global models of DOC export (Mayorga et al., 2010) and DOC exports  
439 quantified for southeastern Alaska (D'Amore et al., 2015a; D'Amore et al., 2016; Stackpoole et  
440 al., 2017), our estimates of freshwater DOC yield from Calvert and Hecate Island watersheds are  
441 in the upper range predicted for the perhumid rainforest region. When compared to watersheds of  
442 similar size, DOC yields from Calvert and Hecate Island watersheds are some of the highest  
443 observed (see reviews in Hope et al., 1994; Alvarez-Cobelas et al., 2012), including DOC yields  
444 from many tropical rivers, despite the fact that tropical rivers have been shown to export very

445 high DOC (e.g., Autuna River, Venezuela, DOC yield= 56,946 kg C km<sup>-2</sup> yr<sup>-1</sup>; Castillo et al.,  
446 2004), and are often regarded as having disproportionately high carbon export compared to  
447 temperate and Arctic rivers (Aitkenhead and McDowell, 2000; Borges et al., 2015). Our  
448 estimates of DOC yield are comparable to, or higher than, previous estimates from high-latitude  
449 catchments of similar size that receive high amounts of precipitation and contain extensive  
450 organic soils and wetlands (e.g. Naiman, 1982 (DOC yield= 48,380 kg C km<sup>-2</sup> yr<sup>-1</sup>); Brooks et  
451 al., 1999 (DOC yield= 20,300 kg C km<sup>-2</sup> yr<sup>-1</sup>); Ågren et al., 2007 (DOC yield= 32,043 kg C km<sup>-2</sup>  
452 yr<sup>-1</sup>)). However, many of these catchments represent low (first or second) order headwater  
453 streams that drain to higher order stream reaches, rather than directly to the ocean. Although  
454 headwater streams have been shown to export up to 90% of the total annual carbon in stream  
455 systems (Leach et al., 2016), significant processing and loss typically occurs during downstream  
456 transit (Battin et al., 2008).

457 Over much of the incised outer coast of the CTR, small rainfall-dominated catchments  
458 contribute high amounts of freshwater runoff to the coastal ocean (Royer, 1982; Morrison et al.,  
459 2012; Carmack et al., 2015). Small mountainous watersheds that discharge directly to the ocean  
460 can exhibit disproportionately high fluxes of carbon relative to watershed size, and in aggregate  
461 may deliver more than 50% of total carbon flux from terrestrial systems to the ocean (Milliman  
462 and Syvitski, 1992; Masiello and Druffel, 2001). Extrapolating our estimate of annual DOC yield  
463 from Calvert and Hecate Island watersheds to the entire hypermaritime subregion of British  
464 Columbia's CTR (29,935 km<sup>2</sup>), generates an estimated annual DOC flux of 0.997 Tg C yr<sup>-1</sup>  
465 (0.721 to 1.305 Tg C yr<sup>-1</sup> for our lowest to highest yielding watersheds, respectively), with the  
466 caveat that this estimate is rudimentary and does not account for spatial heterogeneity in  
467 controlling factors such as wetland extent, topography, and watershed size. Regional

468 comparisons estimate that Southeast Alaska (104,000 km<sup>2</sup>), at the northern range of the CTR,  
469 exports approximately 1.25 Tg C yr<sup>-1</sup> (Stackpoole et al., 2016), while south of the perhumid  
470 CTR, the wet northwestern United States and its associated coastal temperate rainforests export  
471 less than 0.153 Tg C yr<sup>-1</sup> as DOC (reported as TOC, Butman et al., 2016). This suggests that the  
472 hypermaritime coast of British Columbia plays an important role in the export of DOC from  
473 coastal temperate rainforest ecosystems of western North America, in a region that is already  
474 expected to contribute high quantities of DOC to the coastal ocean.

#### 475 **4.2 DOM composition**

476 The composition of stream water DOM exported from Calvert and Hecate Island  
477 watersheds is mainly terrestrial, indicating the production and overall supply of terrestrial  
478 material is sufficient to exceed microbial demand, and thus a relatively abundant supply of  
479 terrestrial DOM is available for export. Values for  $\delta^{13}\text{C}$ -DOC suggest terrestrial carbon sources  
480 from C3 plants and soils were the dominant input to catchment stream water DOM (Finlay and  
481 Kendall, 2007). Measures of  $S_R$  and  $\text{SUVA}_{254}$  were typical of environments that export large  
482 quantities of high molecular weight, highly aromatic DOM such as some tropical rivers (e.g.,  
483 Lambert et al., 2016; Mann et al., 2014), streams draining wetlands (e.g., Ågren et al., 2008,  
484 Austnes et al., 2010), or streams draining small undisturbed catchments comprised of mixed  
485 forest and wetlands (e.g. Wickland et al., 2007; Fellman et al., 2009a; Spencer et al., 2010,  
486 Yamashita et al., 2011). This suggests the majority of the DOM pool is comprised of larger  
487 molecules that have not been extensively chemically or biologically degraded through processes  
488 such as microbial utilization or photodegradation, and therefore are potentially more biologically  
489 available (Amon and Benner, 1996).

490 Biological utilization of DOM is influenced by its composition (e.g. Judd et al., 2006;  
491 Fasching et al., 2014), therefore differences in DOM can alter the downstream fate and  
492 ecological role of freshwater-exported DOM. For example, the majority of the fluorescent DOM  
493 pool was comprised of C1, which is described as humic-like, less-processed terrestrial soil and  
494 plant material (see Table 2). In addition, although the tryptophan-like component C6, represents  
495 a minor proportion of total fluorescence, even a small proteinaceous fraction of the overall DOM  
496 pool can play a major role in overall bioavailability and bacterial utilization of DOM (Berggren  
497 et al., 2010; Guillaumette and Giorgio, 2011). These contributions of stream-exported DOM may  
498 represent a relatively fresh, seasonally-consistent contribution of terrestrial subsidy from streams  
499 to the coastal ecosystem, which in this region is relatively lower in carbon and nutrients  
500 throughout much of the year (Whitney et al., 2005; Johannessen et al., 2008).

#### 501 **4.3. DOC and DOM export: Sources and seasonal variability**

502 On Calvert and Hecate Islands, the relationship between DOC concentration and  
503 discharge varied by watershed (see Supplemental Fig. S6.1), as might be expected given the  
504 known influence of watershed characteristics (e.g., lake area, wetland area, soils, etc) on DOC  
505 concentration and export. However, overall DOC concentrations increased in all watersheds with  
506 both discharge and temperature indicating the overarching drivers of DOC export are the  
507 hydrologic coupling of precipitation and runoff from the landscape with the seasonal production  
508 and availability of DOC (Fasching et al., 2016).

509 Precipitation is a well-established driver of stream DOC export (Alvarez-Cobelas et al.,  
510 2012), particularly in systems containing organic soils and wetlands (Olefeldt et al., 2013; Wallin  
511 et al., 2015; Leach et al., 2016). Frequent, high intensity precipitation events and short residence  
512 times are expected to result in pulsed exports of stream DOC that are rapidly shunted

513 downstream, thus reducing time for in-stream processing (Raymond et al., 2016). Flashy stream  
514 hydrographs indicate that hydrologic response times for Calvert and Hecate Island watersheds  
515 are rapid, presumably as a result of small catchment size, high drainage density, and relatively  
516 shallow soils with high hydraulic conductivity (Gibson et al., 2000; Fitzgerald et al., 2003).  
517 Rapid runoff is presumably accompanied by rapid increases in water tables and lateral movement  
518 of water through shallow soil layers rich in organic matter (Fellman et al., 2009b; D'Amore et  
519 al., 2015b). It appears that on Calvert and Hecate Islands, the combination of high rainfall, rapid  
520 runoff, and abundant sources of DOC from organic-rich wetlands and forests, result in high DOC  
521 fluxes.

522         The relationship between DOC, stream temperature, and discharge indicates that seasonal  
523 dynamics play an important role in the variability of DOC exported from these systems. For  
524 example, DOC concentrations decrease in all watersheds during the wet period of the year, these  
525 decreases are associated with clear changes in DOM composition, such as increasing  $\delta^{13}\text{C-DOC}$ ,  
526  $\text{SUVA}_{254}$ , and decreasing  $S_R$ . This is in contrast with patterns observed during the dry period,  
527 when DOC concentrations gradually increase, while  $\delta^{13}\text{C-DOC}$ ,  $\text{SUVA}_{254}$  decrease. Fluctuations  
528 in DOC and DOM composition occur throughout the wet and the dry season, suggesting that  
529 temperature and runoff – and perhaps other seasonal drivers - are important year-round controls  
530 on DOC concentration as well as certain measures of DOM composition, such as  $\delta^{13}\text{C-DOC}$  and  
531  $S_R$ .

532         The process of “DOC flushing” has been shown to increase stream water DOC during  
533 higher flows in coastal and temperate watersheds (e.g., Sanderman et al., 2009; Deirmendjian et  
534 al., 2017). Flushing can occur through various mechanisms. For example, Boyer et al. (1996)  
535 observed that during drier periods, DOC pools can increase in soils and are then flushed to

536 streams when water tables rise. Rising water tables can establish strong hydraulic gradients that  
537 initiate and sustain prolonged increases in metrics like SUVA<sub>254</sub>, until the progressive drawdown  
538 of upland water tables constrain flow paths (Lambert et al., 2013). DOC concentrations can vary  
539 during flushing in response to changing flow paths, which can shift sources of DOC within the  
540 soil profile from older material in deeper soil horizons to more recently produced material in  
541 shallow horizons (Sanderman et al., 2009), or from changes in the production mechanism of  
542 DOC (Lambert et al., 2013). For example, Sanderman et al. (2009), observed distinct  
543 relationships between discharge and both  $\delta^{13}\text{C}$ -DOC and SUVA<sub>254</sub>, and postulated that during  
544 their rainy season, hillslope flushing shifts DOM sources to more aged soil organic material. In  
545 addition, instream production can also provide a source of DOC, and therefore affect seasonal  
546 variation in DOC concentration and composition (Lambert et al., 2013). The extent of these  
547 effects can shift seasonally; relationships between flow paths and DOC export in rain-dominated  
548 catchments can vary within and between hydrologic periods depending on factors such as the  
549 degree of soil saturation, duration of previous drying and rewetting cycles, soil chemistry, and  
550 DOM source-pool availability (Lambert et al., 2013).

551 Our observations of changes in DOC and DOM related to discharge and stream  
552 temperature suggest that a variety of mechanisms may be important for controlling dynamics of  
553 seasonal export in Pacific hypermaritime watersheds. We observed elevated DOC concentrations  
554 during precipitation events following extended dry periods, suggesting DOC may accumulate  
555 during dry periods and be flushed to streams during runoff events. Increased discharge was  
556 significantly related to  $\delta^{13}\text{C}$ -DOC and  $S_R$ , with higher discharge resulting in more terrestrial-like  
557 DOM. One possible explanation is that hydrologic connectivity increases during higher  
558 discharge as soil conditions become more saturated, therefore promoting the mobilization of



559 DOM from across a wider range of the soil profile (McKnight et al., 2001; Kalbitz et al., 2002).  
560 In addition, the mechanisms of DOC production and sources of DOC appear to shift seasonally.  
561 Relationships between increased temperature and lower values of  $\delta^{13}\text{C}$ -DOC, and higher values  
562 of Freshness Index, C1 and C4, suggest that warmer conditions result in a fresh supply of DOM  
563 exported from terrestrial sources (Fellman et al., 2009a; Fasching et al., 2016). This may  
564 represent a shift in the source of DOM and/or increased contributions from less aromatic, lower  
565 molecular weight material, such as DOM derived from increased terrestrial primary production  
566 (Berggren et al., 2010). Further, fine-scaled investigation into the mechanistic underpinnings of  
567 the relationship between discharge, stream temperature, and DOM, represents a clear priority for  
568 future research in this region.

#### 569 **4.4 Relationships between watershed attributes and exported DOM**

570 Previous studies have implicated wetlands as a major driver of DOM composition (e.g.,  
571 Xenopoulos et al., 2003; Ågren et al., 2008; Creed et al., 2008), however the analysis of  
572 relationships between Calvert and Hecate Island landscape attributes and variation in DOM  
573 composition suggests that controls on DOM composition are more nuanced than being solely  
574 driven by the extent of wetlands. Ågren et al. (2008) found that when wetland area comprised  
575 >10% of total catchment area, wetland DOM was the most significant driver of stream DOM  
576 composition during periods of high hydrologic connectivity. Although wetlands comprise an  
577 average of 37% of our study area, they do not appear to be the single leading driver of variability  
578 in DOC concentration and DOM composition. Other factors, such as watershed slope, the depth  
579 of organic and mineral soil materials, and the presence of lakes also appear to be influence DOC  
580 concentration and DOM composition. The presence of cyptic wetlands (Creed et al., 2003) and

581 limitations of the wetland mapping method could also weaken the link between wetland extent,  
582 DOC, and DOM.

583         In these watersheds, soils with pronounced accumulations of organic matter are not  
584 restricted to wetland ecosystems. Peat accumulation in wetland ecosystems results in the  
585 formation of organic soils (Hemists), where mobile fractions of DOM accumulate under  
586 saturated soil conditions and limited drainage, resulting in the enrichment of poorly  
587 biodegradable, more stable humic acids (Stevenson, 1994; Marschner and Kalbitz, 2003).  
588 Although Hemist soils comprise 27.8% of our study area, Follic Histosols, which form under  
589 more freely drained conditions, such as steeper slopes, occur over an additional 25.7% of the  
590 area (Supplemental S1.2). In freely drained organic soils, high rates of respiration can result in  
591 further enrichment of aromatic and more complex molecules, and this material may be rapidly  
592 mobilized and exported to streams (Glatzel et al., 2003). This suggests the importance of widely  
593 distributed, alternative soil DOM source-pools, such as Follic Histosols and associated Podzols  
594 with thick forest floors on hillslopes, available to contribute high amounts of terrestrial carbon  
595 for export.

596         Although lakes make up a relatively small proportion of the total landscape area, their  
597 influence on DOM export appears to be important. The proportion of lake area can be a good  
598 predictor of organic carbon loss from a catchment since lakes often increase hydrologic  
599 residence times and thus increase opportunities for biogeochemical processing (Algesten et al.,  
600 2004; Tranvik et al., 2009). In our study, watersheds with a larger percentage of lake area  
601 exhibited slower response following rain events (Supplemental Fig. S2.2), lower DOC yields,  
602 and lake area was correlated with parameters that represent greater autochthonous DOM  
603 production or microbial processing such as higher Freshness Index,  $S_R$ , Fluorescence Index, and

604 higher proportions of component C6. In contrast, watersheds with a high percentage of wetlands  
605 contributed DOM that was more allocthonous in composition. Lakes are known to be important  
606 landscape predictors of DOC, as increased residence time enables removal via respiration, thus  
607 reducing downstream exports from lake outlets (Larson et al., 2007). The proximity of wetlands  
608 and lakes to the watershed outlet can also play an important role in the composition of DOM  
609 exports (Martin et al., 2006).

## 610 **5. Conclusions**

611 Previous work has demonstrated freshwater discharge is substantial along the coastal  
612 margin of the North Pacific temperate rainforest, and plays an important role in processes such as  
613 ocean circulation (Royer, 1982; Eaton and Moore, 2010). Our finding that small catchments in  
614 this region contribute high yields of terrestrial DOC to coastal waters suggests that freshwater  
615 inputs may also influence ocean biogeochemistry and food web processes through terrestrial  
616 organic matter subsidies. Our findings also suggest that this region may be currently  
617 underrepresented in terms of its role in global carbon cycling. Currently, there is no region-wide  
618 carbon flux model for the Pacific coastal temperate rainforest or the greater Gulf of Alaska,  
619 which would quantify the importance of this region within the global carbon budget. Our  
620 estimates point to the importance of the hypermaritime outer-coast zone of the CTR, where  
621 subdued terrain, high rainfall, ocean moderated temperatures and poor bedrock have generated a  
622 distinctive ‘bog-forest’ landscape mosaic within the greater temperate rainforest (Banner et al.  
623 2005). However, even within our geographically limited study area, we observed a range of  
624 DOC yields across watersheds. To quantify regional scale fluxes of rainforest carbon to the  
625 coastal ocean, further research will be needed to estimate DOC yields across complex spatial  
626 gradients of topography, climate, hydrology, soils and vegetation. Long term changes in DOC

627 flux have been observed in many places (e.g., Worrall et al., 2004; Borken et al., 2011; Lepistö et  
628 al., 2014; Tank et al., 2016) and continued monitoring of this system will allow us to better  
629 understand the underlying drivers of export and evaluate future patterns in DOC yields. Coupled  
630 with current studies investigating the fate of terrestrial material in ocean food webs, this work  
631 will improve our understanding of coastal carbon patterns, and increase capacity for predictions  
632 regarding the ecological impacts of climate change.

### 633 **Author Contributions**

634 The authors declare that they have no conflict of interest.

635 A.A. Oliver prepared the manuscript with contributions from all authors, designed analysis  
636 protocols, analyzed samples, performed the modeling and analysis for dissolved organic carbon  
637 fluxes, parallel factor analysis of dissolved organic matter composition, and all remaining  
638 statistical analyses. S.E. Tank assisted with designing the study and overseeing laboratory  
639 analyses, crafting the scope of the paper, and determining the analytical approach.

640 I. Giesbrecht led the initial DOC sampling design, helped coordinate the research team, oversaw  
641 routine sampling and data management, and led the watershed characterization.

642 M.C. Korver developed the rating curves, and conducted the statistical analysis of discharge  
643 measurement uncertainties and rating curve uncertainties. W.C. Floyd lead the hydrology  
644 component of this project, selected site locations, installed and designed the hydrometric  
645 stations, and developed the rating curves and final discharge calculations. C. Bulmer and P.  
646 Sanborn collected and analyzed soil field data and prepared the digital soils map of the  
647 watersheds. K.P. Lertzman conceived of and co-led the overall study of which this paper is a  
648 component, helped assemble and guide the team of researchers who carried out this work,  
649 provided input to each stage of the study.

650

651 **Acknowledgements**

652 This work was funded by the Tula Foundation and the Hakai Institute. The authors would like to  
653 thank many individuals for their support, including Skye McEwan, Bryn Fedje, Lawren McNab,  
654 Nelson Roberts, Adam Turner, Emma Myers, David Norwell, and Chris Coxson for sample  
655 collection and data management, Clive Dawson and North Road Analytical for sample  
656 processing and data management, Keith Holmes for creating our maps, Matt Foster for database  
657 development and support, Shawn Hateley for sensor network maintenance, Jason Jackson, Colby  
658 Owen, James McPhail, and the entire staff at Hakai Energy Solutions for installing and  
659 maintaining the sensors and telemetry network, and Stewart Butler and Will McInnes for field  
660 support. Thanks to Santiago Gonzalez Arriola for generating the watershed summaries and  
661 associated data products, and Ray Brunsting for overseeing the design and implementation of the  
662 sensor network and the data management system at Hakai. Additional thanks to Lori Johnson  
663 and Amelia Galuska for soil mapping field assistance, and Francois Guillemette for PARAFAC  
664 consultation. Thanks to Dave D'Amore for inspiring the Hakai project to investigate aquatic  
665 fluxes at the coastal margin and for technical guidance. Lastly, thanks to Eric Peterson and  
666 Christina Munck who provided significant guidance throughout the process of designing and  
667 implementing this study.

668

669 **References**

670 Ågren, A., Buffam, I., Jansson, M. and Laudon, H.: Importance of seasonality and small streams  
671 for the landscape regulation of dissolved organic carbon export, *J. Geophys. Res. Biogeosci.*,  
672 112(G3), doi:10.1029/2006JG000381, 2007.  
673

674 Ågren, A., Buffam, I., Berggren, M., Bishop, K., Jansson, M. and Laudon, H.: Dissolved organic  
675 carbon characteristics in boreal streams in a forest-wetland gradient during the transition  
676 between winter and summer, *J. Geophys. Res. Biogeosci.*, 113(G3), doi:10.1029/2007JG000674,  
677 2008.

678

679 Akaike, H.: Likelihood of a model and information criteria, *J. Econometrics*, 16(1), 3-14,  
680 doi:10.1016/0304-4076(81)90071-3, 1981.

681

682 Aitkenhead, J.A., and McDowell, W.H.: Soil C:N ratio as a predictor of annual riverine DOC  
683 flux at local and global scales, *Global Biogeochem. Cycles*, 14(1), 127–138,  
684 doi:10.1029/1999GB900083, 2000.

685

686 Alaback, P.B.: Biodiversity patterns in relation to climate: The coastal temperate rainforests of  
687 North America, *Ecol. Stud.*, 116, 105–133, doi:10.1007/978-1-4612-3970-3\_7, 1996.

688

689 Algesten, G., Sobek, S., Bergström, A., Ågren, A., Tranvik, L. and Jansson, M.: Role of lakes for  
690 organic carbon cycling in the boreal zone, *Global Change Biol.*, 10(1), 141–147,  
691 doi:10.1111/j.1365-2486.2003.00721.x, 2004.

692

693 Alvarez-Cobelas, M., Angeler, D., Sánchez-Carrillo, S. and Almendros, G.: A worldwide view  
694 of organic carbon export from catchments, *Biogeochemistry*, 107(1-3), 275–293,  
695 doi:10.1007/s10533-010-9553-z, 2012.

696

697 Amon, R.M.W., and Benner, R.: Bacterial utilization of different size classes of dissolved  
698 organic matter, *Limnol. Oceanogr.*, 41, 41-51, 1996.

699

700 Aufdenkampe, A., Mayorga, E., Raymond, P., Melack, J., Doney, S., Alin, S., Aalto, R., and  
701 Yoo, K.: Riverine coupling of biogeochemical cycles between land, oceans, and atmosphere,  
702 *Front. Ecol. Environ.*, 9(1), 53–60, doi:10.1890/100014, 2011.

703

704 Austnes, K., Evans, C.D., Eliot-Laize, C., Naden, P.S., and Old, G.H.: Effects of storm events on  
705 mobilisation and in-stream processing of dissolved organic matter (DOM) in a Welsh peatland  
706 catchment, *Biogeochem.*, 99, 157-173, doi:10.1007/s10533-009-9399-4, 2010.

707

708 Banner, A., LePage, P., Moran, J., and de Groot, A. (Eds.): The HyP3 Project: pattern,  
709 process, and productivity in hypermaritime forests of coastal British Columbia -  
710 a synthesis of 7-year results, Special Report 10, Res. Br., British Columbia Ministry Forests,  
711 Victoria, British Columbia, 142 pp., available at:  
712 <http://www.for.gov.bc.ca/hfd/pubs/Docs/Srs/Srs10.htm>, 2005.

713

714 Battin, T.J., Kaplan, L.A., Findlay, S., Hopkinson, C.S., Marti, E., Packman, A.I., Newbold, D.,  
715 and Sabater, F.: Biophysical controls on organic carbon fluxes in fluvial networks, *Nature*  
716 *Geosci.*, 1, 95–100, 2008.

717

718 Bauer, J.E., Cai, W.J., Raymond, P.A., T.S., Bianchi, Hopkinson, C.S., and Regnier, P.A.G.: The  
719 changing carbon cycle of the coastal ocean, *Nature*, 504(7478), 61-70, doi:10.1038/nature12857,  
720 2013.

721

722 Berggren, M., Laudon, H., Haei, M., Ström, L., and Jansson, M.: Efficient aquatic bacterial  
723 metabolism of dissolved low-molecular-weight compounds from terrestrial sources, *ISME J.*,  
724 doi:10.1038/ismej.2009.120, 2010.

725

726 Boehme, J. and Coble, P.: Characterization of Colored Dissolved Organic Matter Using High-  
727 Energy Laser Fragmentation, *Environ. Sci. Technology*, 34(15), 3283–3290,  
728 doi:10.1021/es9911263, 2000.

729

730 Borcard, D., Gillet, F., and Legendre, P.: *Numerical ecology with R*, Springer, New York,  
731 United States, doi:10.1007/978-1-4419-7976-6, 2011.

732

733 Borken, W., Ahrens, B., Schultz, C. and Zimmermann, L.: Site-to-site variability and temporal  
734 trends of DOC concentrations and fluxes in temperate forest soils, *Global Change Biol.*, 17:  
735 2428–2443, doi:10.1111/j.1365-2486.2011.02390.x, 2011.

736

737 Borges, A.V., Darchambeau, F., Teodoru, C.R., Marwick, T.R., Tamooh, F., Geeraert, N.,  
738 Omengo, F.O., Guérin, F., Lambert, T., Morana, C., Okuku, E., and Bouillon, S.: Globally  
739 significant greenhouse-gas emissions from African inland waters, *Nature Geosci.*, 8, 637–642,  
740 doi:10.1038/ngeo2486, 2015.

741

742 Boyer, E.W., Hornberger, G.M., Bencala, K.E., and McKnight, D.: Overview of a simple model  
743 describing variation of dissolved organic carbon in an upland catchment, *Ecol. Modell.*, 86, 183-  
744 188, 1996.

745

746 Burnham K.P., and Anderson, D.R.: *Model selection and multimodel inference*, 2nd edn.  
747 Springer, New York, 2002.

748

749 Carmack, E., Winsor, P., and William, W.: The contiguous panarctic Riverine Coastal Domain:  
750 A unifying concept, *Prog. Oceanogr.*, 139, 13-23, doi:10.1016/j.pocean.2015.07.014, 2015.

751

752 Castillo, M.M., Allan, J.D., Sinsabaugh, R.L., and Kling, G.W.: Seasonal and interannual  
753 variation of bacterial production in lowland rivers of the Orinoco basin, *Freshwater Biol.*, 49(11),  
754 1400-1414, doi:10.1111/j.1365-2427.2004.01277.x, 2004.

755

756 Clark, J.M., Lane, S.N., Chapman, P.J., and Adamson, J.K.: Export of dissolved organic carbon  
757 from an upland peatland during storm events: Implications for flux estimates, *J. Hydrol.*, 347(3-  
758 4), 438-447, doi: 10.1016/j.jhydrol.2007.09.030, 2007.

759

760 Coble, P., Castillo, C. and Avril, B.: Distribution and optical properties of CDOM in the Arabian  
761 Sea during the 1995 Southwest Monsoon, *Deep Sea Res. Part II, Oceanogr.*, 45(10-11), 2195–  
762 2223, doi:10.1016/S0967-0645(98)00068-X, 1998.

763

764 Cole, J., Prairie, Y., Caraco, N., McDowell, W., Tranvik, L., Striegl, R., Duarte, C., Kortelainen,  
765 P., Downing, J., Middelburg, J. and Melack, J.: Plumbing the Global Carbon Cycle: Integrating  
766 Inland Waters into the Terrestrial Carbon Budget, *Ecosystems*, 10(1), 172–185,  
767 doi:10.1007/s10021-006-9013-8, 2007.

768

769 Cory, R.M., and McKnight, D.M.: Fluorescence spectroscopy reveals ubiquitous presence of  
770 oxidized and reduced quinines in dissolved organic matter, *Environ. Sci. Technol.*, 39, 8142 -  
771 8149, doi:10.1021/es0506962, 2005.

772

773 Creed, I.F., Beall, F.D., Clair, T.A., Dillon, P.J., and Hesslein, R.H.: Predicting export of  
774 dissolved organic carbon from forested catchments in glaciated landscapes with shallow soils,  
775 *Glob. Biogeochem. Cycles*, 22, GB4024, doi:10.1029/2008GB003294, 2008.

776

777 Creed, I.F., Sanford, S.E., Beall, F.D., Molot, L.A., and Dillon, P.J.: Cryptic wetlands:  
778 integrating hidden wetlands in regression models of the export of dissolved organic carbon from  
779 forested landscapes, *Hydrol. Process.*, 17, 3629-3648, 2003.

780

781 D'Amore, D.V., Edwards, R.T., and Biles, F.E.: Biophysical controls on dissolved organic  
782 carbon concentrations of Alaskan coastal temperate rainforest streams, *Aquat. Sci.*,  
783 doi:10.1007/s00027-015-0441-4, 2015a.

784

785 D'Amore, D.V., Edwards, R.T., Herendeen, P.A., Hood, E., and Fellman, J.B.: Dissolved  
786 organic carbon fluxes from hydrogeologic units in Alaskan coastal temperate rainforest  
787 watersheds, *Soil Sci. Soc. Am. J.*, 79:378-388, doi:10.2136/sssaj2014.09.0380, 2015b.

788

789 D'Amore, D.V., Biles, F.E., Nay, M., Rupp, T.S.: Watershed carbon budgets in the southeastern  
790 Alaskan coastal forest region, in: *Baseline and projected future carbon storage and greenhouse-*  
791 *gas fluxes in ecosystems of Alaska*, U.S. Geological Survey Professional Paper, 1826, 196 p.,  
792 2016.

793

794 Dai, M., Yin, Z., Meng, F., Liu, Q. and Cai, W.J.: Spatial distribution of riverine DOC inputs to  
795 the ocean: an updated global synthesis, *Curr. Opin. Sust.*, 4(2), 170–178,  
796 doi:10.1016/j.cosust.2012.03.003, 2012.

797

798 Deirmendjian, L., Loustau, D., Augusto, L., Lafont, S., Chipeaux, C., Poirier, D., and Abril, G.:  
799 Hydrological and ecological controls on dissolved carbon concentrations in groundwater and  
800 carbon export to surface waters in a temperate pine forest watershed, *Biogeosciences*  
801 *Discuss.*, doi:10.5194/bg-2017-90, in review, 2017.

802

803 DellaSala, D.A.: *Temperate and Boreal Rainforests of the World*, Island Press, Washington,  
804 D.C., 2011.

805

806 Emili, L. and Price, J.: Biogeochemical processes in the soil-groundwater system of a forest-  
807 peatland complex, north coast British Columbia, Canada, *Northwest Sci.*, 88, 326–348,  
808 doi:10.3955/046.087.0406, 2013.

809



810 Fasching, C., Behounek, B., Singer, G. and Battin, T.: Microbial degradation of terrigenous  
811 dissolved organic matter and potential consequences for carbon cycling in brown-water streams,  
812 *Sci. Rep.*, 4, 4981, doi:10.1038/srep04981, 2014.  
813

814 Fasching, C., Ulseth, A., Schelker, J., Steniczka, G. and Battin, T.: Hydrology controls dissolved  
815 organic matter export and composition in an Alpine stream and its hyporheic zone, *Limnol.*  
816 *Oceanogr.*, 61(2), 558–571, doi:10.1002/lno.10232, 2016.  
817

818 Fellman, J., Hood, E., D’Amore, D., Edwards, R. and White, D.: Seasonal changes in the  
819 chemical quality and biodegradability of dissolved organic matter exported from soils to streams  
820 in coastal temperate rainforest watersheds, *Biogeochemistry*, 95, 277–293, doi:10.1007/s10533-  
821 009-9336-6, 2009a.  
822

823 Fellman, J., Hood, E., Edwards, R. and D’Amore, D.: Changes in the concentration,  
824 biodegradability, and fluorescent properties of dissolved organic matter during stormflows in  
825 coastal temperate watersheds, *J. Geophys. Res. Biogeosci.*, 114, doi:10.1029/2008JG000790,  
826 2009b.  
827

828 Fellman, J., Hood, E. and Spencer, R.: Fluorescence spectroscopy opens new windows into  
829 dissolved organic matter dynamics in freshwater ecosystems: A review, *Limnol. Oceanogr.*, 55,  
830 24522462, doi:10.4319/lo.2010.55.6.2452, 2010.  
831

832 Fellman, J., Nagorski, S., Pyare, S., Vermilyea, A.W., Scott, D., and Hood, E.: Stream  
833 temperature response to variable glacier cover in coastal watersheds of Southeast Alaska,  
834 *Hydrol. Process.*, 28, 2062-2073, doi:10.1002/hyp.9742, 2014  
835

836 Finlay, J.C., and Kendall, C.: Stable isotope tracing of temporal and spatial variability in organic  
837 matter sources and variability in organic matter sources to freshwater ecosystems, in *Stable*  
838 *Isotopes in Ecology and Environmental Science*, 2, Michener, R., and Lajtha, K. (Eds),  
839 Blackwell Publishing Ltd, Oxford, UK, 283-324, 2007.  
840

841 Fitzgerald, D., Price, J., and Gibson, J.: Hillslope-swamp interactions and flow pathways in a  
842 hypermaritime rainforest, British Columbia, *Hydrol. Process.*, 17, 3005-3022,  
843 doi:10.1002/hyp.1279, 2003.  
844

845 Gibson, J.J., Price, J.S., Aravena, R., Fitzgerald, D.F., and Maloney, D.: Runoff generation in a  
846 hypermaritime bog-forest upland, *Hydrol. Process*, 14, 2711-2730, doi: 10.1002/1099-  
847 1085(20001030)14:15<2711::AID-HYP88>3.0.CO;2-2, 2000.  
848

849 Glatzel, S., Kalbitz, K., Dalva, M., and Moore, T.: Dissolved organic matter properties and their  
850 relationship to carbon dioxide efflux from restored peat bogs, *Geoderma*, 113, 397-411, 2003.  
851

852 Gonzalez Arriola S., Frazer, G.W., Giesbrecht, I.: LiDAR-derived watersheds and their metrics  
853 for Calvert Island, Hakai Institute, doi:dx.doi.org/10.21966/1.15311, 2015.  
854

855 Gorham, E., Lehman, C., Dyke, A., Clymo, D., and Janssens, J.: Long-term carbon sequestration  
856 in North American peatlands, *Quat. Sci. Review*, 58, 77-82, 2012.

857

858 Graeber, D., Gelbrecht, J., Pusch, M., Anlanger, C. and von Schiller, D.: Agriculture has  
859 changed the amount and composition of dissolved organic matter in Central European headwater  
860 streams, *Sci. Total Environ.*, 438, 435–446, doi:10.1016/j.scitotenv.2012.08.087, 2012.

861

862 Green, R.N.: Reconnaissance level terrestrial ecosystem mapping of priority landscape units of  
863 the coast EBM planning area: Phase 3, Prepared for British Columbia Ministry Forests, Lands  
864 and Natural Resource Ops., Blackwell and Associates, Vancouver, Canada, 2014.

865

866 Guillemette, F. and Giorgio, P.: Reconstructing the various facets of dissolved organic carbon  
867 bioavailability in freshwater ecosystems, *Limnol. Oceanogr.*, 56, 734–748,  
868 doi:10.4319/lo.2011.56.2.0734, 2011.

869

870 Hansen, A.M., Kraus, T.E.C., Pellerin, B.A., Fleck, J.A., Downing, B.D., and Bergamaschi,  
871 B.A.: Optical properties of dissolved organic matter (DOM): Effects of biological and photolytic  
872 degradation, *Limnol. Oceanogr.*, 61, 1015-1032, doi:10.1002/lno.10270, 2016.

873

874 Harrell, F.E., Dupont, C., and many others.: Hmisc: Harrell Miscellaneous. R package version  
875 4.0-2. <https://CRAN.R-project.org/package=Hmisc>, 2016.

876

877 Harrison, J., Caraco, N. and Seitzinger, S.: Global patterns and sources of dissolved organic  
878 matter export to the coastal zone: Results from a spatially explicit, global model, *Global*  
879 *Biogeochem. Cycles*, 19, doi:10.1029/2005gb002480, 2005.

880

881 Helms, J., Stubbins, A., Ritchie, J., Minor, E., Kieber, D. and Mopper, K.: Absorption spectral  
882 slopes and slope ratios as indicators of molecular weight, source, and photobleaching of  
883 chromophoric dissolved organic matter, *Limnol. Oceanogr.*, 53, 955–969,  
884 doi:10.4319/lo.2008.53.3.0955, 2008.

885

886 Helton, A., Wright, M., Bernhardt, E., Poole, G., Cory, R. and Stanford, J.: Dissolved organic  
887 carbon lability increases with water residence time in the alluvial aquifer of a river floodplain  
888 ecosystem, *J. Geophys. Res. Biogeosciences*, 120, 693–706, doi:10.1002/2014JG002832, 2015.

889

890 Hoffman, K.M., Gavin, D.G., Lertzman, K.P., Smith, D.J., and Starzomski, B.M.: 13,000 years  
891 of fire history derived from soil charcoal in a British Columbia coastal temperate rain forest,  
892 *Ecosphere*, 7, e01415, doi:10.1002/ecs2.1415, 2016.

893

894 Hope, D., Billett, M.F., and Cresser, M.S.: A review of the export of carbon in river water:  
895 Fluxes and processes, *Environ. Pollut.*, 84(3), 301-324, doi:10.1016/0269-7491(94)90142-2,  
896 1994.

897

898 Hopkinson, C.S., Buffam, I., Hobbie, J., Vallino, J. and Perdue, M.: Terrestrial inputs of organic  
899 matter to coastal ecosystems: An intercomparison of chemical characteristics and bioavailability,  
900 *Biogeochemistry*, 43, 211–234, 1998.

901  
902 Hudson, N., Baker, A. and Reynolds, D.: Fluorescence analysis of dissolved organic matter in  
903 natural, waste and polluted waters-a review, *River Res. Appl.*, 23, 631–649,  
904 doi:10.1002/rra.1005, 2007.

905  
906 Hurvich, C.M., and Tsai, C.: Regression and time series model selection in small samples,  
907 *Biometrika*, 76(2), 297-307, doi:10.2307/2336663, 1989.

908  
909 International Union of Soil Sciences (IUSS) Working Group: World Reference Base for Soil  
910 Resources, International soil classification system for naming soils and creating legends for soil  
911 maps, World Soil Resources Reports No. 106, Food and Agricultural Organization of the United  
912 Nations, Rome, Italy, 2015.

913  
914 ISO Standard 9196: Liquid flow measurement in open channels - Flow measurements under ice  
915 conditions, International Organization for Standardization, available online at [www.iso.org](http://www.iso.org),  
916 1992.

917  
918 ISO Standard 748: Hydrometry - Measurement of liquid flow in open channels using current-  
919 meters or floats, International Organization for Standardization, available online at [www.iso.org](http://www.iso.org),  
920 2007.

921  
922 Johannessen, S.C., Potentier, G., Wright, C.A., Masson, D., and Macdonald, R.W.: Water  
923 column organic carbon in a Pacific marginal sea (Strait of Georgia, Canada), *Mar. Environ. Res.*,  
924 66, S49-S61, doi:10.1016/j.marenvres.2008.07.008, 2008.

925  
926 Johnson, P.C.D.: Extension of Nakagawa & Schielzeth's  $R^2_{GLMM}$  to random slopes models.  
927 *Methods Ecol. Evol.*, DOI: 10.1111/2041-210X.12225, 2014.

928  
929 Johnson, M., Couto, E., Abdo, M. and Lehmann, J.: Fluorescence index as an indicator of  
930 dissolved organic carbon quality in hydrologic flowpaths of forested tropical watersheds,  
931 *Biogeochemistry*, 105, 149–157, doi:10.1007/s10533-011-9595-x, 2011.

932  
933 Judd, K., Crump, B. and Kling, G.: Variation in dissolved organic matter controls bacterial  
934 production and community composition, *Ecology*, 87, 2068–2079, doi:10.1890/0012-  
935 9658(2006)87[2068:VIDOMC]2.0.CO;2, 2006.

936  
937 Kalbitz, K., Schmerwitz, J., Schwesig, D. and Matzner, E.: Biodegradation of soil-derived  
938 dissolved organic matter as related to its properties, *Geoderma*, 113, 273–291,  
939 doi:10.1016/S0016-7061(02)00365-8, 2003.

940  
941 Kling, G., Kipphut, G., Miller, M. and O'Brien, W.: Integration of lakes and streams in a  
942 landscape perspective: the importance of material processing on spatial patterns and temporal  
943 coherence, *Freshwater Biol.*, 43, 477–497, doi:10.1046/j.1365-2427.2000.00515.x, 2000.

944

945 Koehler, A.-K., Murphy, K., Kiely, G. and Sottocornola, M.: Seasonal variation of DOC  
946 concentration and annual loss of DOC from an Atlantic blanket bog in South Western Ireland,  
947 *Biogeochemistry*, 95, 231–242, doi:10.1007/s10533-009-9333-9, 2009.  
948

949 Lakowicz, J.R.: *Principles of Fluorescence Spectroscopy*, 2, Kluwer Academic, New York,  
950 1999.  
951

952 Larson, J.H., Frost, P.C., Zheng, Z., Johnston, C.A., Bridgham, S.D., Lodge, D.M., and  
953 Lamberti, G.A.: Effects of upstream lakes on dissolved organic matter in streams, *Limnol.*  
954 *Oceanogr.*, 52(1), 60-69, doi:10.4319/lo.2007.52.1.0060, 2007.  
955

956 Leighty, W.W., Hamburg, S.P., and Caouette, J.: Effects of management on carbon sequestration  
957 in forest biomass in Southeast Alaska, *Ecosystems*, 9, 1051, doi:10.1007/s10021-005-0028-3,  
958 2006.  
959

960 Lalonde, K., Middlestead, P., G elinas, Y.: Automation of <sup>13</sup>C/<sup>12</sup>C ratio measurement for  
961 freshwater and seawater DOC using high temperature combustion, *Limnol. Oceanogr. Methods*,  
962 12, 816-829, doi:10.4319/lom.2014.12.816, 2014.  
963

964 Lambert, T., Bouillon, S., Darchambeau, F., Massicotte, P., and Borges, A.V.: Shift in the  
965 chemical composition of dissolved organic matter in the Congo River network, *Biogeosci.*, 13,  
966 5405-5420, doi:10.5194/bg-13-5405-2016, 2016.  
967

968 Leach, J., Larsson, A., Wallin, M., Nilsson, M. and Laudon, H.: Twelve year interannual and  
969 seasonal variability of stream carbon export from a boreal peatland catchment, *J. Geophys. Res.*  
970 121, 1851–1866, doi:10.1002/2016JG003357, 2016.  
971

972 Legendre, P., and Durand, S.: rdaTest, Canonical redundancy analysis, R package version 1.11,  
973 available at <http://adn.biol.umontreal.ca/~numerica/ecology/Rcode/>, 2014.  
974

975 Lepist o, A., Futter, M.N. and Kortelainen, P.: Almost 50 years of monitoring shows that climate,  
976 not forestry, controls long-term organic carbon fluxes in a large boreal watershed, *Glob. Change*  
977 *Biol.*, 20, 1225–1237, doi:10.1111/gcb.12491, 2014.  
978

979 Liaw, A., and Wiener, M.: Classification and Regression by randomForest, *R News*, 2(3), 18-22,  
980 2002.  
981

982 Lochmuller, C.H., Saavedra, S.S.: Conformational changes in a soil fulvic acid measured by time  
983 dependent fluorescence depolarization, *Anal. Chem.*, 38, 1978-1981, 1986.  
984

985 Lorenz, D., Runkel, R., and De Cicco, L.: rloadest, River Load Estimation, R package version  
986 0.4.2, available at <https://github.com/USGS-R/rloadest>, 2015.  
987

988 Ludwig, W., Probst, J. and Kempe, S.: Predicting the oceanic input of organic carbon by  
989 continental erosion, *Global Biogeochem. Cycles*, 10, 23–41, doi:10.1029/95GB02925, 1996.  
990

991 Mann, P.J., Spencer, R.G.M., Dinga, B.J., Poulsen, J.R., Hernes, P.J., Fiske, G., Salter, M.E.,  
992 Wang, Z.A., Hoering, K.A., Six, J., and Holmes, R.M.: The biogeochemistry of carbon across a  
993 gradient of streams and rivers within the Congo Basin, *J. Geophys. Res. Biogeosci.*, 119, 687-  
994 702, doi:10.1002/2013JG002442, 2014.

995  
996 Marschner, B., and Kalbitz, K.: Controls on bioavailability and biodegradability of dissolved  
997 organic matter in soils, *Geoderma*, 113, 211–235, 2003.

998  
999 Martin, S.L., and Soranno, P.A.: Lake landscape position: Relationships to hydrologic  
1000 connectivity and landscape features, *Limnol. Oceanogr.*, 51(2), 801-814,  
1001 doi:10.4319/lo.2006.51.2.0801, 2006.

1002  
1003 Masiello, C.A., and Druffel, E.R.M.: Carbon isotope geochemistry of the Santa Clara River,  
1004 *Global Biogeochem. Cycles*, 15, 407-416, doi:10.1029/2000GB001290, 2001.

1005  
1006 Mayorga, E., Seitzinger, S., Harrison, J., Dumont, E., Beusen, A., Bouwman, A.F., Fekete, B.,  
1007 Kroeze, C. and Dreht, G.: Global Nutrient Export from WaterSheds 2 (NEWS 2): Model  
1008 development and implementation, *Environ. Model. Softw.*, 25, 837–853,  
1009 doi:10.1016/j.envsoft.2010.01.007, 2010.

1010  
1011 McClelland, J., Townsend-Small, A., Holmes, R., Pan, F., Stieglitz, M., Khosh, M. and Peterson,  
1012 B.: River export of nutrients and organic matter from the North Slope of Alaska to the Beaufort  
1013 Sea, *Water Resour. Res.*, 50, 1823–1839, doi:10.1002/2013WR014722, 2014.

1014  
1015 McKnight, D., Boyer, E., Westerhoff, P., Doran, P., Kulbe, T. and Andersen, D.:  
1016 Spectrofluorometric characterization of dissolved organic matter for indication of precursor  
1017 organic material and aromaticity, *Limnol. Oceanogr.*, 46, 38–48, doi:10.4319/lo.2001.46.1.0038,  
1018 2001.

1019  
1020 McLaren, D., Fedje, D., Hay, M.B., Mackie, Q., Walker, I.J., Shugar, D.H., Eamer, J.B.R., Lian,  
1021 O.B., and Neudorf, C.: A post-glacial sea level hinge on the central Pacific coast of Canada,  
1022 *Quat. Sci. Review.*, 97, 148-169, 2014.

1023  
1024 Meybeck, M.: Carbon, nitrogen, and phosphorus transport by world rivers, *Am. J. Sci.*, 282, 401-  
1025 450, Available from: <http://earth.geology.yale.edu/~ajs/1982/04.1982.01.Maybeck.pdf>, 1982.

1026  
1027 Milliman, J.D., and Syvitski J.P.M.: Geomorphic tectonic control of sediment discharge to the  
1028 ocean: The importance of small mountainous rivers, *J. Geol.*, 100, 525-544, 1992.

1029  
1030 Moore, R.D.: Introduction to salt dilution gauging for streamflow measurement part III: Slug  
1031 injection using salt in solution, *Streamline Watershed Management Bulletin*, 8(2), 1-6, 2005.

1032  
1033 Morrison, J., Foreman, M.G.G., and Masson, D.: A method for estimating monthly freshwater  
1034 discharge affecting British Columbia coastal waters, *Atmosphere-Ocean*, 50, 1-8,  
1035 doi:10.1080/07055900.2011.637667, 2012.

1036  
1037 Mulholland, P. and Watts, J.: Transport of organic carbon to the oceans by rivers of North  
1038 America: a synthesis of existing data, *Tellus*, 34, 176–186, doi:10.1111/j.2153-  
1039 3490.1982.tb01805.x, 1982.  
1040  
1041 Murphy, K., Stedmon, C., Graeber, D. and Bro, R.: Fluorescence spectroscopy and multi-way  
1042 techniques. *PARAFAC, Anal. Methods*, 5, 6557–6566, doi:10.1039/C3AY41160E, 2013.  
1043  
1044 Murphy K., Stedmon, C., Wenig, P., Bro, R.: OpenFluor- A spectral database of auto-  
1045 fluorescence by organic compounds in the environment, *Anal. Methods*, 6, 658-661,  
1046 DOI:10.1039/C3AY41935E, 2014.  
1047  
1048 Naiman, R.J.: Characteristics of sediment and organic carbon export from pristine boreal forest  
1049 watersheds, *Can. J. Fish. Aquat. Sci.*, 39(12), 1699-1718, doi:10.1139/f82-226, 1982.  
1050  
1051 Nakagawa, S., and Schielzeth, H.: A general and simple method for obtaining  $R^2$  from  
1052 generalized linear mixed-effects models, *Methods Ecol. Evol.*, 4(2): 133-  
1053 142. DOI: 10.1111/j.2041-210x.2012.00261.x, 2013.  
1054  
1055 Olefeldt, D., Roulet, N., Giesler, R. and Persson, A.: Total waterborne carbon export and DOC  
1056 composition from ten nested subarctic peatland catchments- importance of peatland cover,  
1057 groundwater influence, and inter-annual variability of precipitation patterns, *Hydrol. Process.*,  
1058 27, 2280-2294, doi:10.1002/hyp.9358, 2013.  
1059  
1060 Pinheiro, J., Bates, D., DebRoy, S., Sarkar, D., and R Core Team: *nlme: Linear and Nonlinear*  
1061 *Mixed Effects Models*, R package version 3.1-128, 2016.  
1062  
1063 Pojar, J., Klinka, K., and Demarchi, D.A.: Chapter 6, Coastal Western Hemlock Zone, in:  
1064 *Special Report Series 6, Ecosystems of British Columbia*, Meidiner, D., and Pojar, J. (Eds.),  
1065 Ministry of Forests, British Columbia, Victoria, 330 p., 1991.  
1066  
1067 Poulin, B., Ryan, J. and Aiken, G.: Effects of iron on optical properties of dissolved organic  
1068 matter, *Environ. Sci. Technol.*, 48, 10098–106, doi:10.1021/es502670r, 2014.  
1069  
1070 R Core Team, R: A language and environment for statistical computing, R Foundation for  
1071 Statistical Computing, Vienna, Austria, <http://www.R-project.org/>, 2013.  
1072  
1073 Raymond, P., Saiers, J. and Sobczak, W.: Hydrological and biogeochemical controls on  
1074 watershed dissolved organic matter transport: pulse-shunt concept, *Ecology*, 97, 5-16,  
1075 doi:10.1890/14-1684.1, 2016.  
1076  
1077 Regnier, P., Friedlingstein, P., Ciais, P., Mackenzie, F., Gruber, N., Janssens, I., Laruelle, G.,  
1078 Lauerwald, R., Luysaert, S., Andersson, A., Arndt, S., Arnosti, C., Borges, A., Dale, A.,  
1079 Gallego-Sala, A., Godd ris, Y., Goossens, N., Hartmann, J., Heinze, C., Ilyina, T., Joos, F.,  
1080 LaRowe, D., Leifeld, J., Meysman, F., Munhoven, G., Raymond, P., Spahni, R., Suntharalingam,

1081 P. and Thullner, M.: Anthropogenic perturbation of the carbon fluxes from land to ocean, *Nat.*  
1082 *Geosci.*, 6, 597–607, doi:10.1038/ngeo1830, 2013.

1083

1084 Roddick, J.R.: *Geology, Rivers Inlet-Queens Sound, British Columbia, Open File 3278,*  
1085 *Geological Survey of Canada, Ottawa, Canada, 1996.*

1086

1087 Royer, T.C., Coastal fresh water discharge in the northeast, Pacific, *J. Geophys. Res.*, 87, 2017-  
1088 2021, 1982.

1089

1090 Runkel, R.L., Crawford, C.G., and Cohn, T.A.: *Load Estimator (LOADEST): A FORTRAN*  
1091 *program for estimating constituent loads in streams and rivers, U.S. Geological Survey*  
1092 *Techniques and Methods Book 4, Chapter A5, 65 pp., 2004.*

1093

1094 Sanderman, J., Lohse, K.A., Baldock, J.A., and Amundson, R.: Linking soils and streams:  
1095 Sources and chemistry of dissolved organic matter in a small coastal watershed, *Water Resour.*  
1096 *Res.*, 45, W03418, doi:10.1029/2008WR006977, 2009.

1097

1098 Spencer, R., Butler, K. and Aiken, G.: Dissolved organic carbon and chromophoric dissolved  
1099 organic matter properties of rivers in the USA, *J. Geophys. Res. Biogeosciences*, 117(G03001),  
1100 doi:10.1029/2011JG001928, 2012.

1101

1102 Spencer, R.G., Hernes, P.J, Ruf, R., Baker, A., Dyda, R.Y., Stubbins, A., and Six, J.: Temporal  
1103 controls on dissolved organic matter and lignin biogeochemistry in a pristine tropical river,  
1104 Democratic Republic of Congo, *J. Geophys. Res.*, 115, G03013, doi:10.1029/2009JG001180,  
1105 2010.

1106

1107 Stackpoole, S.M., Butman, D.E., Clow, D.W., Verdin, K.L., Gaglioti, B., and Striegl, R.: Carbon  
1108 burial, transport, and emission from inland aquatic ecosystems in Alaska, in: *Baseline and*  
1109 *projected future carbon storage and greenhouse-gas fluxes in ecosystems of Alaska, Zhiliang, Z.,*  
1110 *and David, A. (Eds.), U.S. Geological Survey Professional Paper, 1826, 196 p., 2016.*

1111

1112 Stackpoole, S.M., Butman, D.E., Clow, D.W., Verdin, K.L., Gaglioti, B.V., Genet, H., and  
1113 Striegl, R.G.: *Inland waters and their role in the carbon cycle of Alaska, Ecol. Appl., Accepted*  
1114 *Author Manuscript, doi: 10.1002/eap.1552, 2017.*

1115

1116 Stedmon, C. and Bro, R.: Characterizing dissolved organic matter fluorescence with parallel  
1117 factor analysis: a tutorial, *Limnol. Oceanogr. Methods*, 6, 572–579,  
1118 doi:10.4319/lom.2008.6.572b, 2008.

1119

1120 Stedmon, C. and Markager, S.: Tracing the production and degradation of autochthonous  
1121 fractions of dissolved organic matter by fluorescence analysis, *Limnol. Oceanogr.*, 50(5), 1415–  
1122 1426, doi:10.4319/lo.2005.50.5.1415, 2005.

1123

1124 Stedmon, C., Markager, S., Bro, R., Stedmon, C., Markager, S. and Bro, R.: Tracing dissolved  
1125 organic matter in aquatic environments using a new approach to fluorescence spectroscopy, *Mar.*  
1126 *Chem.*, doi:10.1016/S0304-4203(03)00072-0, 2003.

1127  
1128 Stevenson, F.J.: *Humus Chemistry: Genesis, Composition, Reactions*, 2, Jon Wiley and Sons  
1129 Inc., New York, United States of America, 1994.  
1130  
1131 Symonds, M.R.E., and Moussalli, A.: A brief guide to model selection, multimodel inference,  
1132 and model averaging in behavioural ecology using Akaike's information criterion, *Behav. Ecol.*  
1133 *Sociobiol.*, 65:13-21, DOI: 10.1007/s00265-010-1037-6, 2011.  
1134  
1135 Tallis, H.: Kelp and rivers subsidize rocky intertidal communities in the Pacific Northwest  
1136 (USA), *Marine Ecology Progress Series*, 389, 8596, doi:10.3354/meps08138, 2009.  
1137  
1138 Tank, S., Raymond, P., Striegl, R., McClelland, J., Holmes, R., Fiske, G. and Peterson, B.: A  
1139 land-to-ocean perspective on the magnitude, source and implication of DIC flux from major  
1140 Arctic rivers to the Arctic Ocean, *Global Biogeochem. Cycles*, 26, GB4018,  
1141 doi:10.1029/2011GB004192, 2012.  
1142  
1143 Tank, S., Striegl, R.G., McClelland, J.W., and Kokelij, S.V.: Multi-decadal increases in  
1144 dissolved organic carbon and alkalinity flux from the Mackenzie drainage basin to the Arctic  
1145 Ocean, *Environ. Res. Lett.*, 11(5), doi:10.1088/1748-9326/11/5/054015, 2016.  
1146  
1147 Thompson, S.D., Nelson, T.A., Giesbrecht, I., Frazer, G., and Saunders, S.C.: Data-driven  
1148 regionalization of forested and non-forested ecosystems in coastal British Columbia with LiDAR  
1149 and RapidEye imagery, *Appl. Geogr.*, 69, 35–50, doi: 10.1016/j.apgeog.2016.02.002,  
1150 2016.  
1151  
1152 Trant, A.J., Nijland, W., Hoffman, K.M., Mathews, D.L., McLaren, D., Nelson, T.A.,  
1153 Starzomski, B.M.: Intertidal resource use over millennia enhances forest productivity, *Nature*  
1154 *Commun.*, 7, 12491, doi: 10.1038/ncomms12491, 2016.  
1155  
1156 van Hees, P., Jones, D., Finlay, R., Godbold, D. and Lundström, U.: The carbon we do not see-  
1157 the impact of low molecular weight compounds on carbon dynamics and respiration in forest  
1158 soils: a review, *Soil Biol. Biochem.*, 37, 1–13, doi:10.1016/j.soilbio.2004.06.010, 2005.  
1159  
1160 Wallin, M., Weyhenmeyer, G., Bastviken, D., Chmiel, H., Peter, S., Sobek, S. and Klemetsson,  
1161 L.: Temporal control on concentration, character, and export of dissolved organic carbon in two  
1162 hemiboreal headwater streams draining contrasting catchments, *J. Geophys. Res. Biogeosci.* 120,  
1163 832–846, doi:10.1002/2014jg002814, 2015.  
1164  
1165 Wang, T., Hamann, A., Spittlehouse, D.L., and Murdock, T.Q.: ClimateWNA- High resolution  
1166 spatial climate data for Western North America, *J. Appl. Meteorol. Climatol.*, 51, 16-29,  
1167 doi:dx.doi.org/10.1175/JAMC-D-11-043.1, 2012.  
1168  
1169 Weishaar, J.L., Aiken, G.R., Bergamaschi, B.A., Fram, M.S., Fujii, R. and Mopper, K.:  
1170 Evaluation of specific ultraviolet absorbance as an indicator of the chemical composition and



1171 reactivity of dissolved organic carbon, *Environ. Sci. Technol.*, 37, 4702–4708,  
1172 doi:10.1021/es030360x, 2003.

1173

1174 Whitney, F.A., Crawford, W.R. and Harrison, P.J.: Physical processes that enhance nutrient  
1175 transport and primary productivity in the coastal and open ocean of the subarctic NE  
1176 Pacific, *Deep Sea Research Part II: Topical Studies in Oceanography*, 52, 681–706, 2005.

1177

1178 Wickland, K., Neff, J., and Aiken, G.: Dissolved Organic Carbon in Alaskan Boreal Forest:  
1179 Sources, Chemical Characteristics, and Biodegradability, *Ecosystems*, 10, 1323-1340, 2007.

1180

1181 Wilson, H.F. and Xenopoulos, M.A.: Effects of agricultural land use on the composition of  
1182 fluvial dissolved organic matter, *Nat. Geosci.*, 2, 37–41, doi:10.1038/ngeo391, 2009.

1183

1184 Wolf, E.C., Mitchell, A.P., and Schoonmaker, P.K.: *The Rain Forests of Home: An Atlas of*  
1185 *People and Place*, Ecotrust, Pacific GIS, Inforain, and Conservation International, Portland,  
1186 Oregon, 24 pp., available at: [http://www.inforain.org/pdfs/ctrf\\_atlas\\_orig.pdf](http://www.inforain.org/pdfs/ctrf_atlas_orig.pdf), 1995.

1187

1188 Worrall, F., Burt, T., and Adamson, J.: Can climate change explain increases in DOC flux from  
1189 upland peat catchements?, *Sci. Total. Environ.*, 326, 95–112,  
1190 doi:10.1016/j.scitotenv.2003.11.022, 2004.

1191

1192 Xenopoulos, M.A., Lodge, D.M., Frentress, J., Kreps, T.A., Bridgham, S.D., Grossman, E., and  
1193 Jackson, C.J.: Regional comparisons of watershed determinants of dissolved organic carbon in  
1194 temperate lakes from the Upper Great Lakes region and selected regions globally, *Limnol.*  
1195 *Oceanogr.*, 48(6), 2321-2334, 2003.

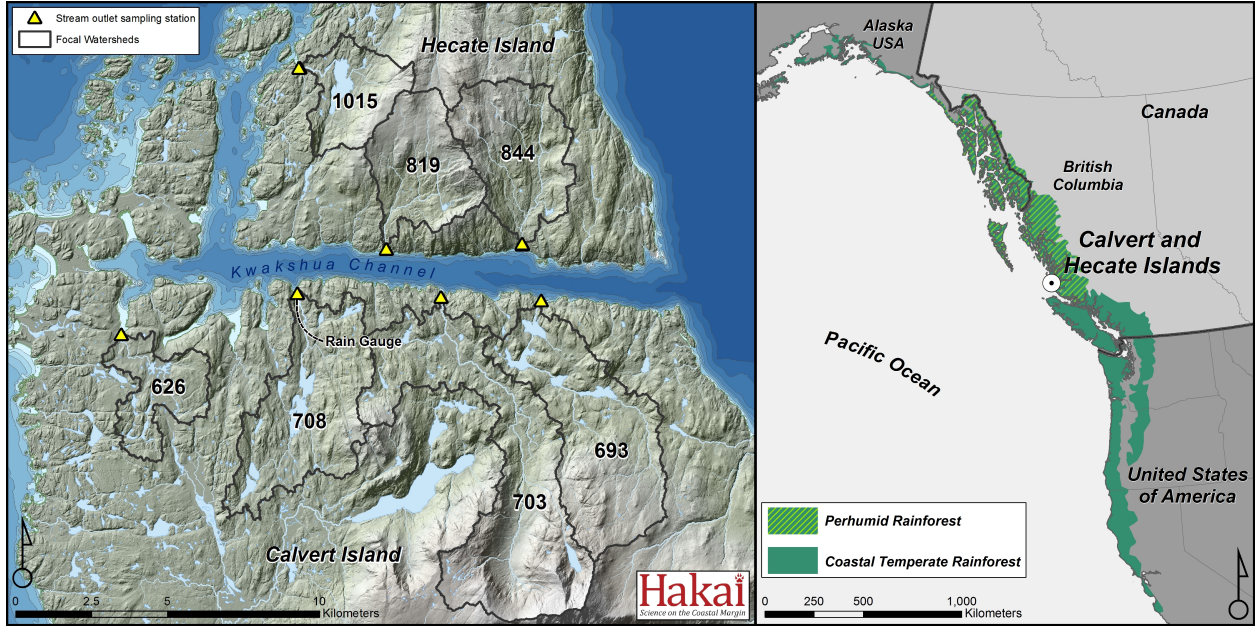
1196

1197 Yamashita, Y. and Jaffé, R.: Characterizing the Interactions between Trace Metals and Dissolved  
1198 Organic Matter Using Excitation–Emission Matrix and Parallel Factor Analysis, *Environ. Sci.*  
1199 *Technol.*, 42, 7374–7379, doi:10.1021/es801357h, 2008.

1200

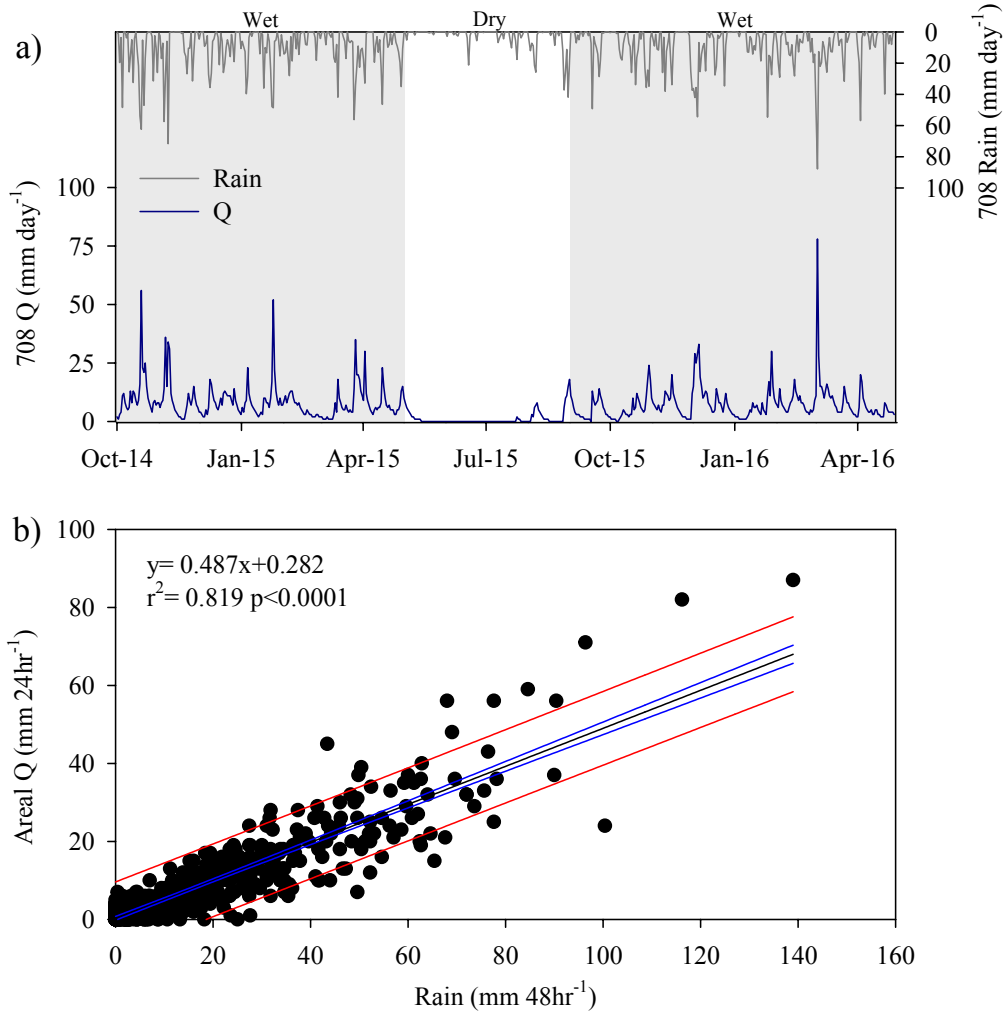
1201 Yamashita, Y., Kloeppel, B., Knoepp, J., Zausen, G. and Jaffé, R.: Effects of Watershed History  
1202 on Dissolved Organic Matter Characteristics in Headwater Streams, *Ecosystems*, 14, 1110–1122,  
1203 doi:10.1007/s10021-011-9469-z, 2011.

1204 **Figure 1.** The location of Calvert Island, British Columbia, Canada, within the perhumid region  
1205 of the coastal temperate rainforest (right) and the study area on Calvert and Hecate Islands,  
1206 including the seven study watersheds, corresponding stream outlet sampling stations, and  
1207 location of the rain gauge (left). Characteristics of individual watersheds are described in Table  
1208 1.  
1209



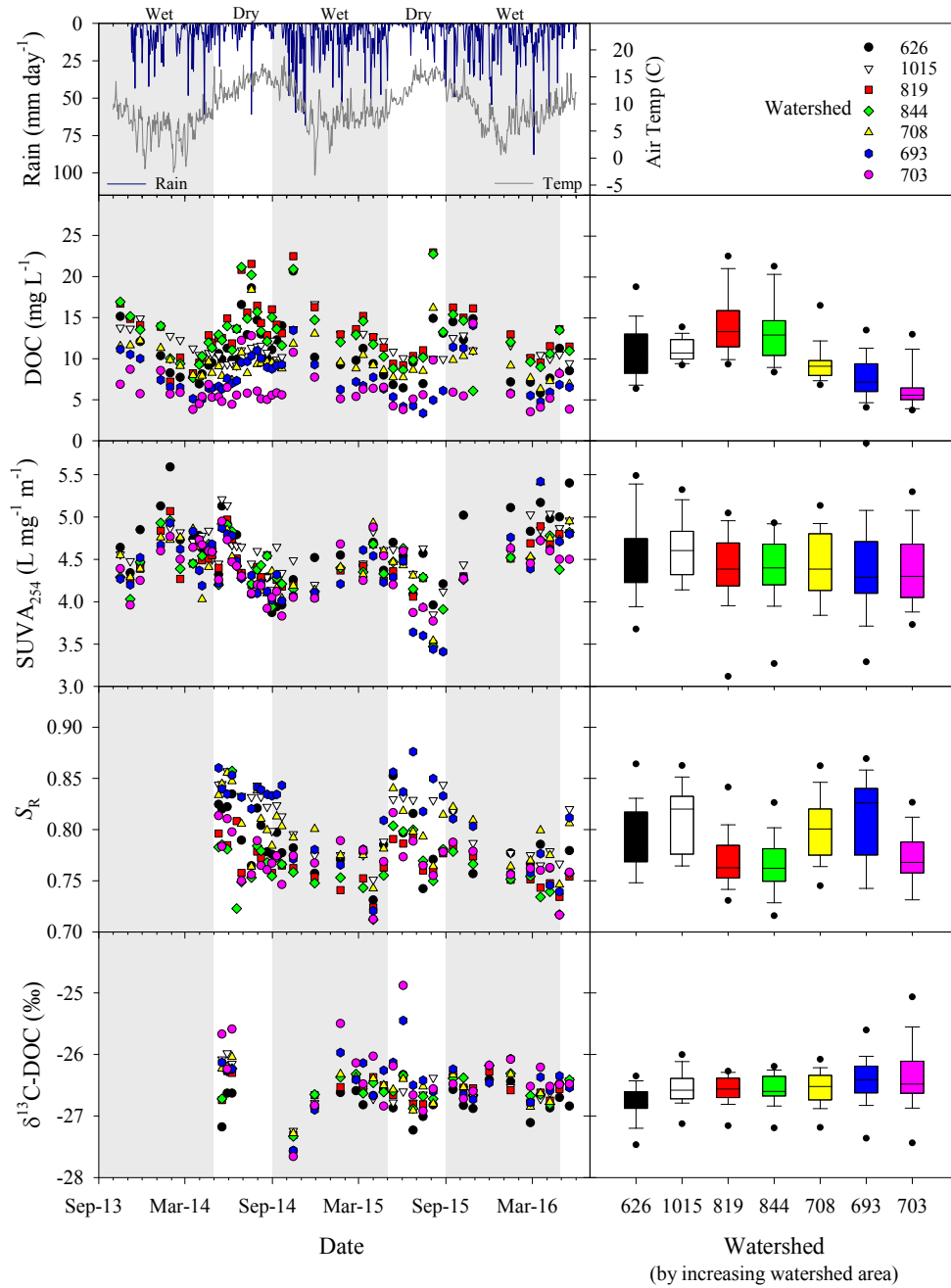
1210  
1211  
1212  
1213  
1214  
1215  
1216  
1217  
1218  
1219  
1220  
1221  
1222  
1223  
1224  
1225  
1226  
1227  
1228  
1229  
1230  
1231

1232 **Figure 2.** Hydrological patterns typical of watersheds located in the study area (a) the  
 1233 hydrograph and precipitation record from Watershed 708 for the study period of October 1,  
 1234 2015-April 30, 2016. Grey shading indicates the wet period (September 1-April 30) and the  
 1235 unshaded region indicates the dry period (May 1-August 30) (b) Correlation of daily (24 hour)  
 1236 areal runoff (discharge of all watersheds combined) to 48 hour total rainfall recorded at  
 1237 watershed 708. For the period of study, comparisons of daily runoff to 48-hr rainfall  
 1238 (runoff:rainfall mean= 0.92, std  $\pm$ 0.27) indicated rapid discharge response to rainfall.



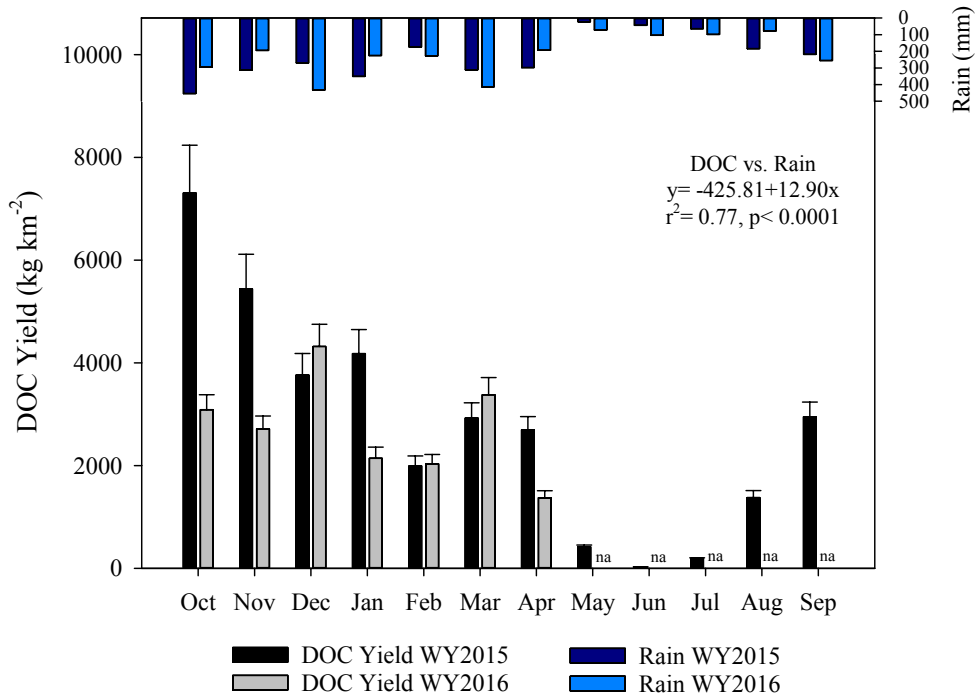
1239  
 1240  
 1241  
 1242

1243 **Figure 3.** Seasonal (timelines, by date) and spatial (boxplots, by watershed) patterns in DOC  
 1244 concentration and DOM composition for stream water collected at the outlets of the seven study  
 1245 watersheds on Calvert and Hecate Islands. Boxes represent the 25<sup>th</sup> and 75<sup>th</sup> percentile, while  
 1246 whiskers represent the 5<sup>th</sup> and 95<sup>th</sup> percentile. Daily precipitation and annual temperature are  
 1247 shown in the top left panel. Grey shading indicates the wet period (September 1-April 30) and  
 1248 the unshaded region indicates the dry period of each water year.  
 1249



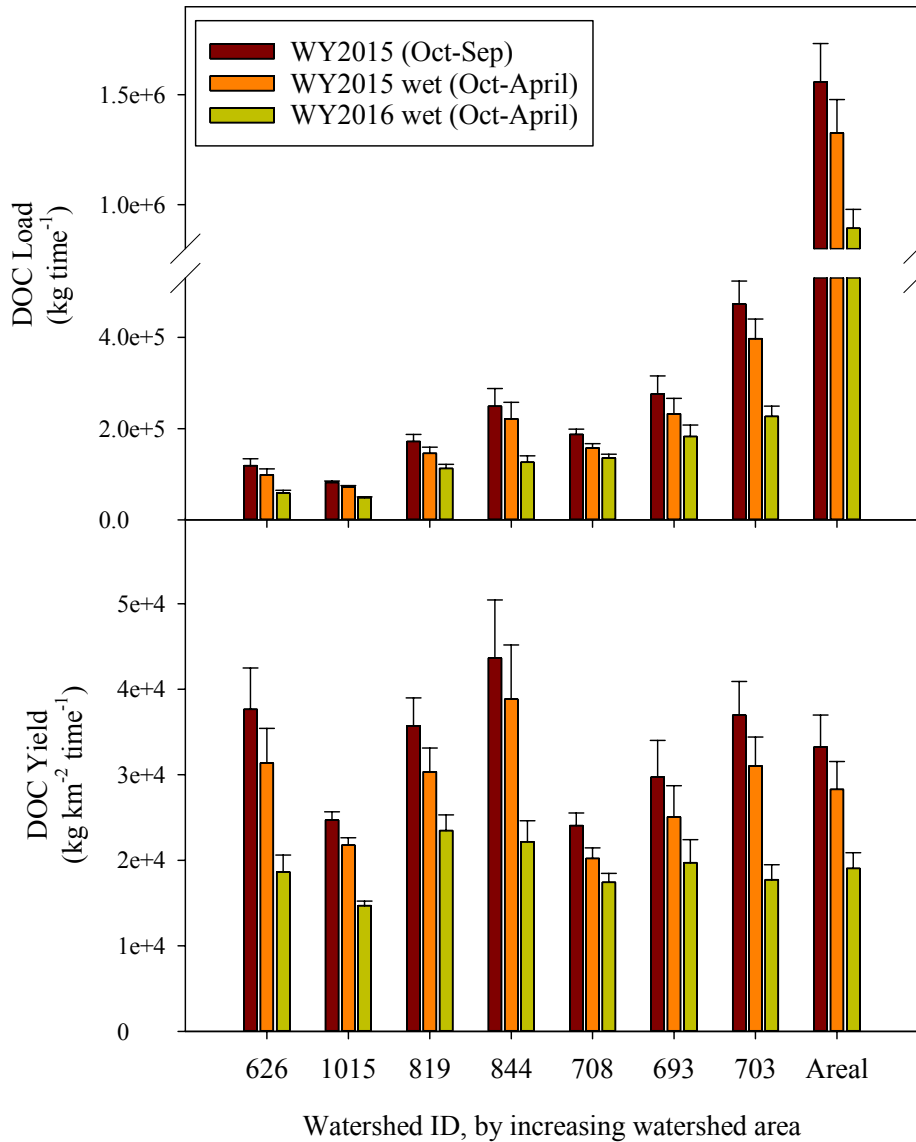
1250

1251 **Figure 4.** Monthly areal DOC yields and precipitation for water year 2015 (WY2015) and the  
 1252 wet period (October 1-April 30) of water year 2016 (WY2016). Error bars represent standard  
 1253 error. Total rain and DOC yield were significantly correlated ( $r^2 = 0.77$ ) and months of higher  
 1254 rain produced higher DOC yields. In WY2015, the majority of DOC export (~94% of annual  
 1255 flux) occurred during the wet period (~88% of annual precipitation).



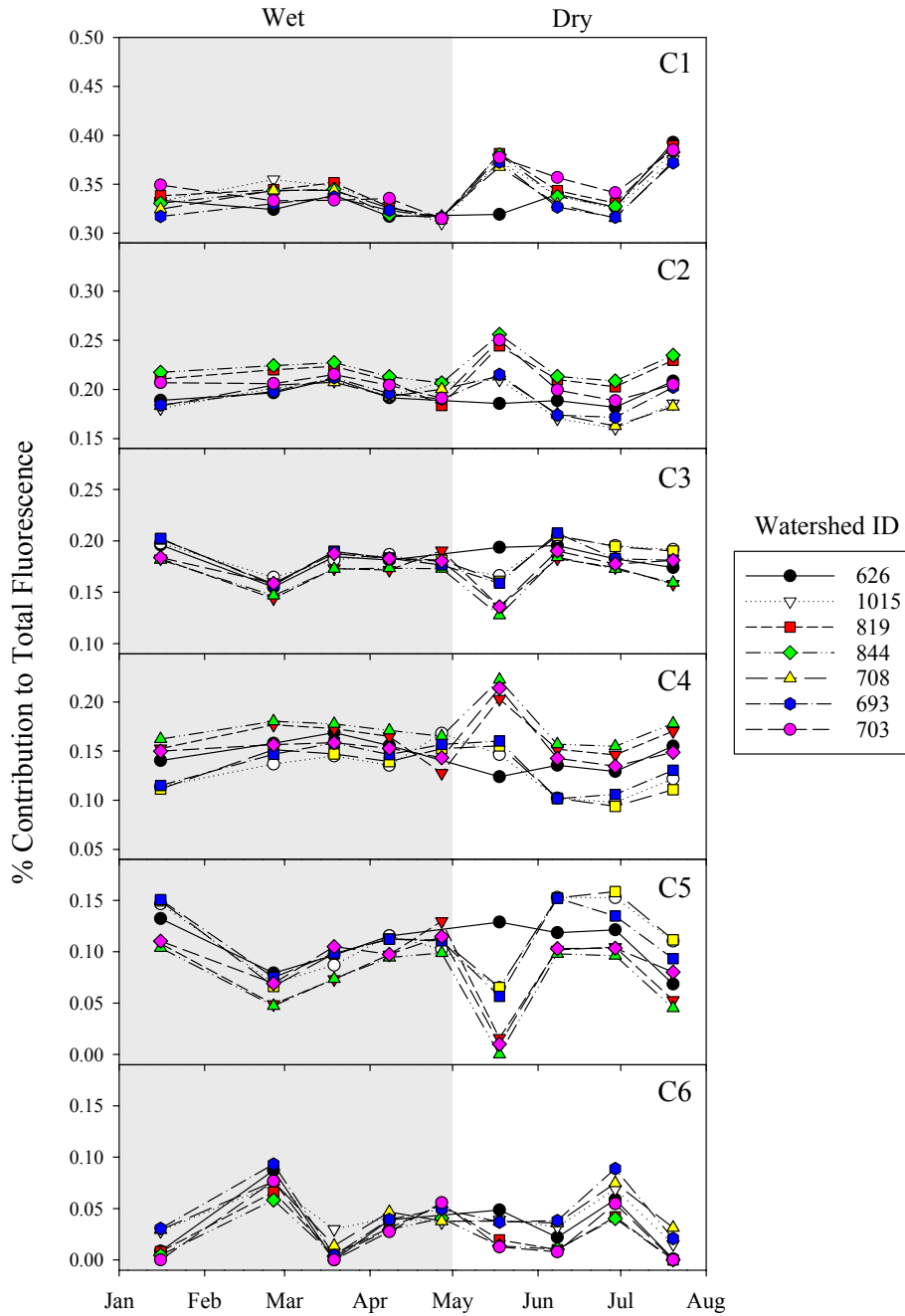
1256  
 1257  
 1258  
 1259  
 1260  
 1261  
 1262  
 1263  
 1264  
 1265  
 1266  
 1267  
 1268  
 1269  
 1270  
 1271  
 1272  
 1273

1274 **Figure 5:** DOC fluxes and yields for the seven study watersheds and the total area of study  
 1275 (“areal”, all watersheds combined) on Calvert and Hecate Islands for water year 2015 (WY2015;  
 1276 Oct 1 - Sep 30), and October 1- April 30 of the wet period for water year 2015 (WY2015 wet)  
 1277 and water year 2016 (WY2016 wet). Because DOC yields were only available for September in  
 1278 WY2015, this month was excluded from the wet period totals in order to make similar  
 1279 comparisons between years. Error bars represent standard error.



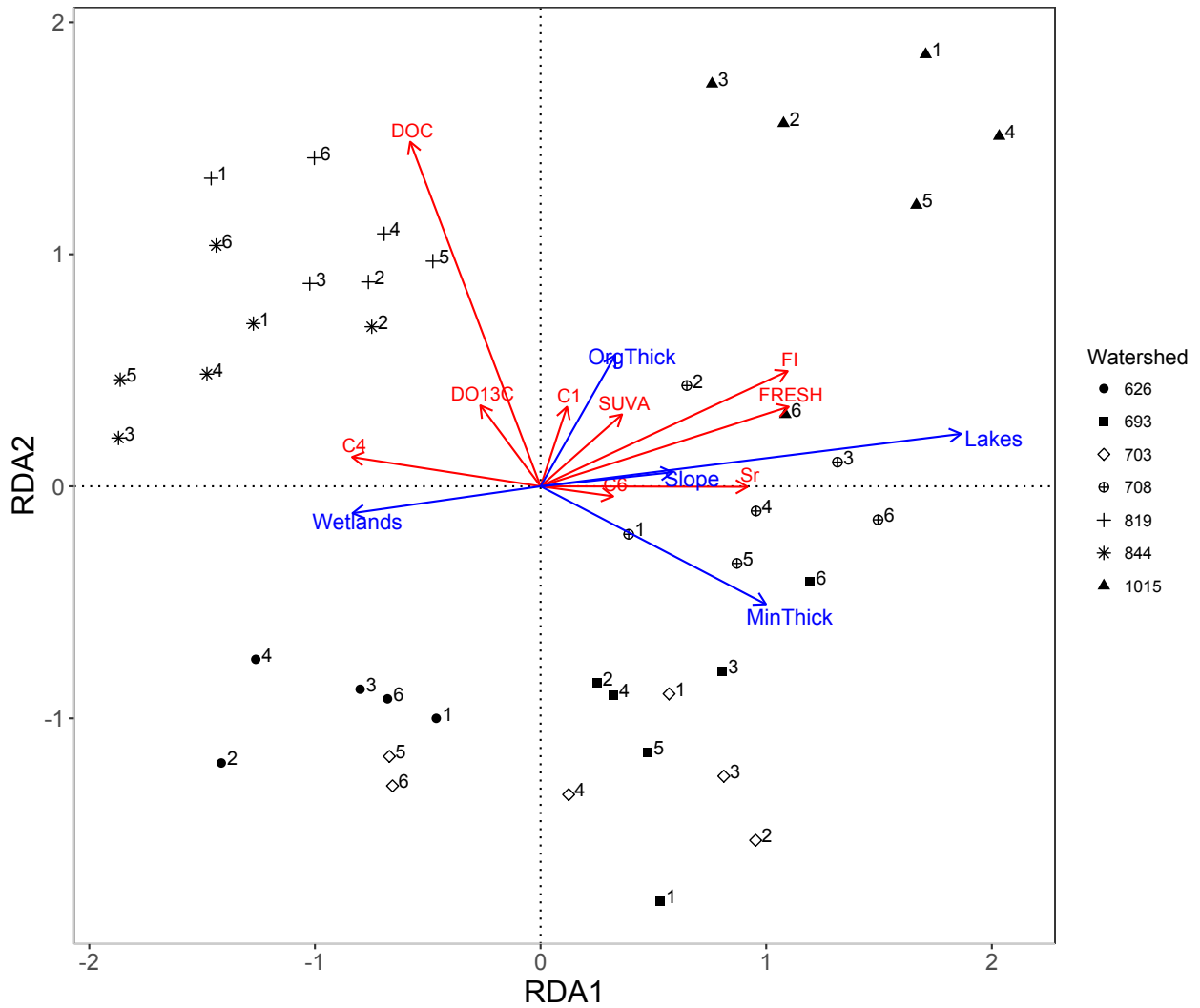
1280 **Figure 6:** Percent contribution of the six components identified in parallel factor analysis  
 1281 (PARAFAC) for samples collected every three weeks from January-July, 2016 from the seven  
 1282 study watersheds on Calvert and Hecate Islands. The grey shading indicates the wet period and  
 1283

1284 the unshaded region indicates the dry period. Note that while the y-axis for each panel has a  
1285 range of 20%, the max and min for each y-axis varies by panel.



1286  
1287 **Figure 7:** Results from the partial-Redundancy analysis (RDA; type 2 scaling) of DOC  
1288 concentration and DOM composition versus watershed characteristics. Angles between vectors  
1289 represent correlation, i.e., smaller angles indicate higher correlation. Symbols represent different

1290 watersheds, and numbers on symbols represent the sample month in 2016: 1= January, 2=  
 1291 February, 3= March, 4= early April, 5= late April, and 6= May.  
 1292



1293



1294 **Table 1:** Watershed characteristics, discharge, DOC concentrations, and DOC yields for the seven study watersheds on Calvert and  
 1295 Hecate Islands. Additional details on the methods used to determine watershed characteristics can be found in Supplemental Material.

Water- shed	Area (km <sup>2</sup> )	Avg. Slope (%)	Lakes (% Area)	Wetlands (% Area)	Avg. Depth Organic Soils (cm)	Avg. Depth Mineral Soils (cm)	Total Q Yield* (mm)	DOC* <sup>a</sup> (mg L <sup>-1</sup> )	Q- weighted Avg. DOC* (mg L <sup>-1</sup> )	DOC Annual Yield <sup>b</sup> WY2015* (Mg C km <sup>-2</sup> )	DOC Monthly Yield <sup>b</sup> Wet Season** (Mg C km <sup>-2</sup> )	DOC Monthly Yield <sup>b</sup> Dry Season*** (Mg C km <sup>-2</sup> )
626	3.2	21.7	4.7	48.0	39.4 ±24.3	30.8 ±8.3	3673	11.0 ±3.5	15.3	37.7 (31.9 – 44.2)	3.59 (3.05 – 4.18)	0.62 (0.49 – 0.77)
1015	3.3	34.2	9.1	23.8	39.5 ±17.2	33.7 ±8.6	3052	11.2 ±1.6	12.9	24.7 (23.6 – 25.8)	2.56 (2.45 – 2.78)	0.27 (0.25 – 0.28)
819	4.8	30.1	0.3	50.2	37.9 ±19.1	29.8 ±5.7	3066	14.0 ±3.5	19.3	35.7 (31.7 – 40.2)	3.80 (3.37 – 5.10)	0.57 (0.48 – 0.67)
844	5.7	32.5	0.3	35.2	35.4 ±18.0	29.1 ±6.4	4129	13.1 ±3.6	15.9	43.6 (34.2 – 54.9)	4.24 (3.36 – 5.30)	0.54 (0.36 – 0.77)
708	7.8	28.5	7.5	46.3	36.2 ±19.7	29.9 ±6.0	3805	9.5 ±2.4	10.9	24.1 (22.2 – 26.0)	2.67 (2.46 – 4.07)	0.38 (0.34 – 0.43)
693	9.3	30.2	4.4	42.8	35.4 ±16.1	30.2 ±6.4	5866	7.7 ±2.5	8.4	29.7 (25.9 – 34.0)	3.19 (2.79 – 4.94)	0.41 (0.32 – 0.52)
703	12.8	40.3	1.9	24.3	37.3 ±16.5	35.8 ±13.4	6058	6.3 ±2.6	9.0	37.0 (32.5 – 42.0)	3.48 (3.07 – 4.02)	0.64 (0.52 – 0.77)
All	46.9	32.7	3.7	37.1	37.4 ±17.7	32.2 ±9.2	4730	10.4 ±3.8	11.1	33.3 (28.9 – 38.1)	3.35 (2.94 – 4.40)	0.50 (0.41 – 0.62)

\* Calculated for water year 2015 (WY2015; Oct 1, 2014-Sep 30, 2015)  
 \*\* Wet period average monthly yield calculated from October-April and September, WY2015 and October-April, WY2016  
 \*\*\* Dry period average monthly yield calculated from May-August, WY2015  
<sup>a</sup> Mean ± standard deviation  
<sup>b</sup> Total ± 95% confidence interval

1297 **Table 2:** Spectral composition for the six fluorescence components identified using PARAFAC, including excitation (Ex.) and  
 1298 emission (Em.) peak values, percent composition across all samples, and likely structure and characteristics of the fluorescent  
 1299 component based on previous studies.

Component	Ex. (nm)	Em. (nm)	% Composition <sup>a</sup>	Potential structure/Characteristics	Previous studies with comparable results
C1	315	436	34.1 ±2.2 (31.1-39.3)	Humic-like, less processed terrestrial, high molecular weight, widespread but highest in wetland and forest environment	Garcia et al. 2015(C1); Graeber et al. 2012(C1); Walker et al. 2014(C1); Yamashita et al. 2011(C1); Cory & McKnight, 2005(C1)
C2	270/ 380	484	20.2 ±1.9 (16.1-25.6)	Humic-like, resembles fulvic acid, widespread, high molecular weight terrestrial	Stedmon and Markager, 2005(C2); Stedmon et al. 2003(C3); Cory & McKnight, 2005(C5)
C3	270	478	17.8 ±1.8 (12.8-20.8)	Humic-like, highly processed terrestrial; suggested as refractory	Stedmon & Markager, 2005(C1); Yamashita et al. 2010(C2)
C4	305/ 435	522	14.8 ±2.6 (9.4-22.3)	Not commonly reported, similarities to fulvic-like, contributed from soils	Lochmuller & Saavedra, 1986(E)
C5	325	442	9.8 ±3.5 (0.0-15.9)	Aquatic humic-like from terrestrial environments; autochthonous, microbial produced; may be photoproduced	Boehme & Coble, 2000(Peak C); Coble et al. 1998(Peak C); Stedmon et al., 2003(C3)
C6	285	338	3.4 ±2.5 (0.0-9.3)	Amino acid-like/Tryptophan-like. Freshly added from land, autochthonous. Rapidly photodegradable	Murphy et al. 2008(C7); Shutova et al. 2003(C4); Stedmon et al. 2007(C7); Yamashita et al. 2003(C5)

<sup>a</sup> Mean ± stdev (min-max) from all samples

1300